Meeting agricultural and environmental water demand in endorheic irrigated river basins
A simulation-optimization approach applied to the Urmia Lake basin in Iran

Dehghanipour, Amir Hossein; Schoups, Gerrit; Zahabiyoun, Bagher; Babazadeh, Hossein

DOI
10.1016/j.agwat.2020.106353

Publication date
2020

Document Version
Accepted author manuscript

Published in
Agricultural Water Management

Meeting agricultural and environmental water demand in endorheic irrigated river basins: a simulation-optimization approach applied to the Urmia Lake basin in Iran

Amir Hossein Dehghanipour[a,*,1], Gerrit Schoups[b], Bagher Zahabiyoun[a,*], Hossein Babazadeh[c]

[a] *Department of Water Management, School of Civil Engineering, Iran University of Science and Technology, Tehran, Iran*
[b] *Department of Water Management, Faculty of Civil Engineering and Geosciences, Delft University of Technology, Delft, The Netherlands*
[c] *Department of Water Science and Engineering, Science and Research Branch, Islamic Azad University, Tehran, Iran*

[*] Corresponding author address: Department of Water Management, School of Civil Engineering, Iran University of Science and Technology, Narmak, Tehran, Iran, Postal Code: 16846-13114.
E-mail: A.Dehghanipour@tudelft.nl (A.H. Dehganipour), Bagher@iust.ac.ir (B. Zahabiyoun)

[1]Present address: Department of Water Management, Faculty of Civil Engineering and Geosciences, Delft University of Technology, Stevinweg 1, 2628CN, Delft, Netherlands. Tel:+31618838382

Highlights

- Simulation-optimization approach for water management in irrigated endorheic basins
- Spatially distributed simulation of surface water and groundwater resources
- Multi-objective optimization to meet environmental and agricultural water demand
- Conjunctive use and time-variable environmental flow requirements to tackle droughts
- Sustainable water management strategies for the Lake Urmia basin

Abstract

Competition for water between agriculture and the environment is a growing problem in irrigated regions across the globe, especially in endorheic basins with downstream freshwater lakes impacted by upstream irrigation withdrawals. This study presents and applies a novel simulation-optimization (SO) approach for identifying water management strategies in such settings. Our approach combines three key features for increased exploration of strategies. First, minimum environmental flow requirements are treated as a decision variable in the optimization model, yielding more flexibility than existing approaches that either treat it as a precomputed constraint or as an objective to be maximized. Second, conjunctive use is included as a management option by using dynamically coupled surface water (WEAP) and groundwater (MODFLOW) simulation models. Third, multi-objective optimization is used to yield entire Pareto sets of water management strategies that trade off between meeting environmental and agricultural water demand. The methodology is applied to the irrigated Miyandoab Plain, located upstream of endorheic Lake Urmia in Northwestern Iran. Results identify multiple strategies, i.e., combinations of minimum environmental flow requirements, deficit irrigation, and crop selection, that simultaneously increase environmental flow (up to 16%) and agricultural profit (up to 24%) compared to historical conditions. Results further show that significant temporary drops in agricultural profit occur during droughts when long-term profit is maximized, but that this can be avoided by increasing groundwater pumping capacity and temporarily reducing the lake's minimum environmental flow requirements. Such a strategy is feasible during moderate droughts when resulting declines in groundwater and lake water levels fully recover after each drought. Overall, these results demonstrate the usefulness and flexibility of the methodology in identifying a range of potential water management strategies in complex irrigated endorheic basins like the Lake Urmia basin.

Keywords: *Environmental flow requirement; Conjunctive use; WEAP; MODFLOW; Multi-Objective Optimization; Drought.*

1. Introduction

Irrigated agriculture is the largest consumer of water resources, accounting for approximately 70% of all freshwater extraction from surface water (SW) and groundwater (GW) resources (Malano and Davidson, 2009; Molden, 2013; Pang et al., 2014, 2013; Singh, 2014). Large agricultural water demand competes with other water demands, in particular environmental flow requirements to sustain natural ecosystems (Jägermeyr et al., 2017; Malano and Davidson, 2009; Pang et al., 2014; Xue et al., 2017). Environmental flow requirement is defined as river flow that is necessary to sustainably maintain ecological health of natural ecosystems, such as wetlands and lakes (Arthington et al., 2018; Smakhtin et al., 2006; Yasi and Ashori, 2017). In many parts of the world, increased water consumption for irrigation has led to mounting pressure on available water resources to meet environmental flow requirements and has resulted in growing conflicts between agricultural and environmental water demand (Dunn et al., 2003; Xue et al., 2017). These conflicts are exacerbated by climate change, drought, and water mismanagement, especially in arid and semi-arid regions (Mancosu et al., 2015; Valipour, 2015; Valipour et al., 2015). Many of the adverse effects of decreasing environmental water flow have led to the degradation of natural aquatic bodies, such as lakes, wetlands, and oases (Sisto, 2009).

Endorheic river basins, usually located in arid and semi-arid regions, are particularly sensitive to competition between agricultural and environmental water demand (Wang et al., 2018). Rivers in endorheic basins do not discharge into the ocean but rather in terminal lakes whose water supplies are sensitive to upstream water extractions and to natural climatic variations such as droughts (Wang et al., 2018). Therefore, maintaining and sustaining environmental flow requirements is a high priority in these basins (Yapiyev et al., 2017) and conflict between agricultural demand and environmental flow requirements in endorheic basins, especially during droughts, has been a focus of various studies (Bai et al., 2012; Chunyu et al., 2019). During the 20th and 21st centuries, SW extraction for irrigated agriculture significantly increased in endorheic river basins, especially in arid and semi-arid regions. Furthermore, the adverse impact of climate change and drought in these regions reduced downstream outflow from rivers, resulting in shrinking and drying up of terminal lakes (Cai and Rosegrant, 2004; Chunyu et al., 2019; Farrokhzadeh et al., 2020; Rumbaur et al., 2015). For instance, the surface area of Lake Chad that is located in the most extensive African endorheic basin, shrank by 90% over the last 40 years (Lemoalle et al., 2012; Yapiyev et al., 2017), while the surface area of Lake Aral in Central Asia decreased by 75% from 1975 to 2007 (Bai et al., 2011; Pritchard, 2017; Yapiyev et al., 2017).

Tharme (2003) reviewed existing methods for calculating environmental flow requirements worldwide. The results of this study indicate that 207 different methodologies exist for calculating environmental flow requirements. A disadvantage of these methods is that other water demands that may exist in the basin, e.g. agricultural water demand, are not taken into account which means that the calculated environmental flow requirements are difficult to achieve in practice and be accepted by stakeholders (Barbier et al., 2009; Mainuddin et al., 2007; O'Keeffe, 2009; Pang et al., 2014; Wei et al., 2009).

A more holistic approach considers environmental flow requirements and agricultural water demand together. This path has been explored by various studies. For instance, Munoz-Hernandez et al. (2011) developed a simulation model to investigate the impact of three alternative environmental water allocation strategies on agricultural profits in the Rio Yaqui basin, Mexico. Other studies used a simulation-optimization (SO) model to find water allocation strategies that simultaneously meet environmental flow requirements and water demand from agriculture and other users (see Table S1). A first distinction among these studies relates to the way minimum environmental flow requirements are estimated: either fixed based on historical streamflow records (e.g., Xevi and Khan, 2005), treated as a function of reservoir water storage (e.g. (Anghileri et al., 2013)), or set to a fixed fraction of river discharge (e.g., Fallah-Mehdipour et al., 2020, 2018; Hu et al., 2016). The latter approach is known as the Tennant method (Tennant, 1976). A second distinction among existing SO studies relates to how environmental flow requirements are included in the optimization model: either as a firm constraint (e.g., Anghileri et al., 2013; Hu et al., 2016; Pulido-Velazquez et al., 2008; Xevi and Khan, 2005), or as an objective function to be maximized (e.g., Fallah-Mehdipour et al., 2020, 2018; Yang and Yang, 2014).

Building on these previous studies, this paper investigates application of SO modeling for resolving competition between environmental flows and agricultural demand in the 1524 km^2 Miyandoab Plain, an irrigated plain in the Urmia Lake Basin, a cold-semi-arid endorheic basin in the northwest of Iran. There are several complex water problems in the Miyandoab Plain due to drought and water mismanagement. Overuse of irrigation in the basin coupled with a recent drought has resulted in decreased environmental flows to Lake Urmia and led to continued shrinking of the lake (Hosseini-Moghari et al., 2018; Moshir Panahi et al., 2020; Schulz et al., 2020). As such, environmental flow requirements for Urmia lake are in direct competition with agricultural water demand. In this regard, the Iranian government has established the Urmia Lake Restoration Program (ULRP) to explore strategies of water consumption reduction and increased efficiency and productivity in the agricultural sector (Shadkam et al., 2016). However, strategies should be designed so that farmers do not suffer income losses. A previous study by Ahmadzadeh et al. (2016) has shown that improvements in irrigation efficiency have little effect in an endorheic basin like the Lake Urmia basin, suggesting the need for other strategies such as changes in crop acreage and crop patterns, and the application of deficit irrigation for decreasing agricultural water consumption and increasing total inflow to the lake (Ahmadzadeh et al., 2016). An additional strategy for resolving temporary water shortage during droughts that has not yet been explored in the Miyandoab Plain consists of conjunctive use of SW and GW resources (Tian et al., 2015), a strategy that has been applied successfully in other regions (e.g., Peralta et al., 1995; Karamouz et al., 2004; Xevi and Khan, 2005; Schoups et al., 2005; Schoups et al., 2006; Safavi et al., 2010; Singh and Panda, 2013; Seo et al., 2018).

The goal of our study is to present a novel SO approach for reconciling competing agricultural and environmental water demands, and apply this methodology for finding potential water management strategies that meet environmental flow requirements to Urmia lake while improving and enhancing the agricultural economy in the upstream Miyandoab Plain. Our study contributes both novel methodology and novel insights into water management in the application case study. In terms of methodology, our paper extends existing studies in at least three different ways. First, while previous SO approaches included environmental flow either as constraint or as objective function in the optimization, here we introduce and test an alternative approach that treats minimum environmental flow requirements as a separate decision variable in the optimization. This approach introduces additional flexibility for finding better water management strategies. Second, our SO model includes both SW and GW components, and as such provides a larger solution space for exploring sustainable water management strategies, e.g. strategies where agriculture increases GW use to reduce SW extractions and meet environmental SW flow requirements. The hydrologic module in our SO model is based on a recently developed WEAP-MODFLOW model of the Miyandoab Plain (Dehghanipour et al., 2019) that includes coupled water balances for all relevant system components, i.e. the root zone, surface water reservoir, river, canals, and the underlying aquifer. Third, multi-objective optimization is used to yield entire Pareto sets of water management strategies that trade-off between meeting environmental and agricultural water demand. In terms of application, our study builds on the recommendations of (Ahmadzadeh et al., 2016) by investigating new strategies for solving the water management problems in Miyandoab Plain that include changes in crop acreage, changes in crop pattern, and application of deficit irrigation.

The paper is divided into five sections. Section 2 introduces the study area, i.e. the Miyandoab Plain in the Urmia Lake basin. Section 3 presents the simulation-optimization model, including a discussion of the hydrologic, agronomic, and economic modules of the simulation model, as well as a description of the decision variables, constraints, and objective functions of the optimization model. Section 4 provides results of the simulation-optimization model for identifying sustainable water allocation strategies that meet agricultural water demand and environmental flow requirements in the Miyandoab Plain. Section 5 summarizes conclusions of the study.

2. Case study

2.1. GW and SW resources, hydrology and hydrogeology

The Miyandoab Plain is an agricultural region located in the northwest of Iran in the Urmia basin (Fig. 1.a), between the Zagros mountains, the Sahand mountains, and Lake Urmia. The region has a semi-arid-cold climate and average annual precipitation of ~290mm, most of which falls from October to May. Annual temperature and reference evapotranspiration average 14°C and 1170 mm, respectively. The population of the Miyandoab Plain equals 255,841 and consists of 70,251 households, with 64% employment in the agricultural sector (Ministry of Energy of Iran, 2016).

The Miyandoab Plain is divided into 21 agricultural zones (Fig. 1.b) which are characterized as either “internal” (with irrigation and drainage canals) or “external” (without irrigation and drainage canals). The total area of all agricultural zones is approximately 100,000 hectares, consisting of orchards (42%) and crops (52%). Orchards consist of apple, grapes, stone-fruits, almond, and conifer trees, which are cultivated from March to October. Crops include wheat, maize, alfalfa, sugar beet, and tomato, each with their own distinctive growing season (Fig. S1). Crops and orchards are irrigated using a combination of SW and GW resources.

The SW system consists of main rivers and their tributaries, reservoirs, and irrigation and drainage canals. The main rivers are Zarrineh Rood, Simineh Rood, Mordaq-Chai, Lilan-Chai, and Quri-Chai, with average annual runoff of 1460, 326, 75, 64, and 41 MCM, respectively (Fig. 1.b). Zarrineh Rood and

Simineh Rood are the most important rivers in Urmia Basin: they provide more than 50% of total annual environmental flows into Urmia Lake (Ghaheri et al., 1999). The biggest reservoir in the Urmia basin, Bukan reservoir, is located on the Zarrineh Rood river (Fig. 1.a) and has a total storage volume that was increased in the year 2008 from 650 to 808 MCM, with 130 MCM of dead storage. SW releases from Bukan reservoir are conveyed to the internal zones via the Norozloo diversion dam and a network of primary irrigation canals (Fig. 1.b).

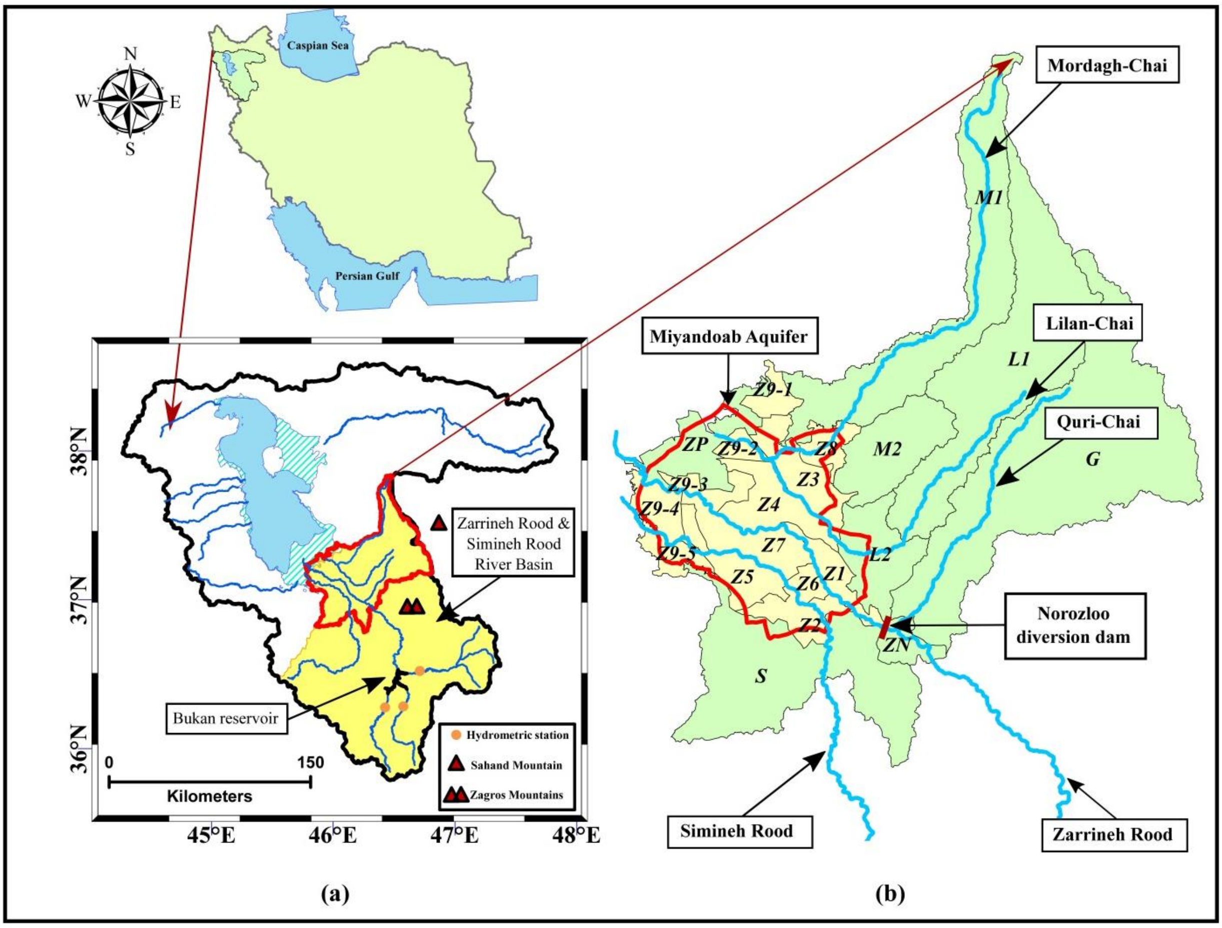

Fig. 1: Location of the study area (a) Miyandoab Plain in the Urmia basin, Iran (b) Agricultural zones in Miyandoab Plain and Miyandoab aquifer. Internal and external zones are shown in yellow and green, respectively.

The internal agricultural zones are underlain by the Miyandoab aquifer (Fig. 1.b). The aquifer is unconfined, and has a small specific yield (on average about 0.035). Twenty-two thousand (22,000) wells with a total annual capacity of approximately 140 MCM are operational in Miyandoab aquifer to supply additional water for irrigation.

Land slope of the internal zones is very low, and irrigation and drainage canals and pumping wells have been extensively developed in the internal zones. These facilities have led to cultivation of most of the land in the internal zones. External zones, on the other hand, consist of mountains and foothills without extensive aquifers. Therefore, agricultural land in the external zones is concentrated along rivers and is irrigated using SW from river diversions and GW from local shallow groundwater along rivers.

2.2. Historical hydrologic droughts in Miyandoab Plain

Fig. S2 shows a time series of annual river discharge upstream of Bukan reservoir (Fig. 1.a), and Fig. 2 shows the corresponding Streamflow Drought Index (SDI), calculated according to Nalbantis and Tsakiris (2009). These data show multi-year droughts (negative SDI) from 1999 to 2002 and from 2006 to 2013. In comparison, the period before 1998 was markedly wetter. Table 1 further indicates that 1999, 2000, 2001, and 2008 were the driest years in the region. Upstream river discharge for these years was 31% of the average upstream river discharge during 1984-2013. These reductions in upstream inflow directly increase competition between sustaining downstream environmental flow to Lake Urmia and sustaining the agricultural economy in Miyandoab Plain. Our goal is to explore water management strategies that alleviate this competition, especially during droughts when water supplies are limited.

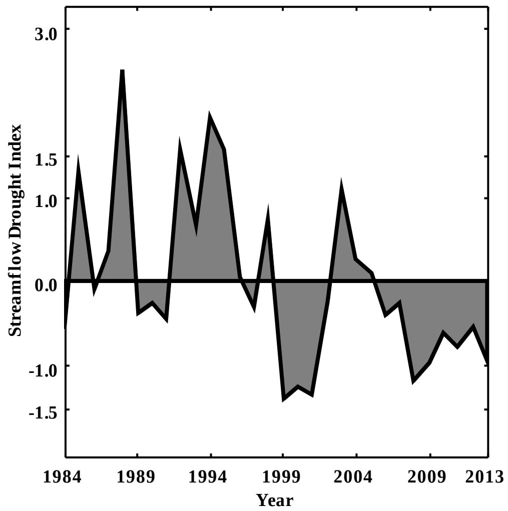

Fig. 2: Annual time series of Streamflow Drought Index (SDI) for upstream inflow into Bukan reservoir

Table 1: Classification of hydrologic drought years in Miyandoab Plain based on the SDI (Nalbantis and Tsakiris, 2009) in Fig. 2

Classification	Identifier	Criterion	Years of occurrence
Non-drought	**HD1**	**0.0 ≤ SDI**	**1985, 1987, 1988, 1992, 1993, 1994, 1995, 1996, 1998, 2003, 2004, 2005**
Mild drought	**HD2**	**-1.0 ≤ SDI < 0.0**	**1984, 1986, 1989, 1990, 1991, 1997, 2002, 2006, 2007, 2009, 2010, 2011, 2012, 2013**
Moderate drought	**HD3**	**-1.5 ≤ SDI < -1**	**1999, 2000, 2001, 2008**
Severe drought	**HD4**	**-2.0 ≤ SPI < -1.5**	**---**
Extreme drought	**HD5**	**SDI < -2.0**	**---**

2.3. Current and proposed crop pattern in the Miyandoab Plain

As mentioned in the introduction, the ULRP has developed scenarios for the reduction of water consumption in the agricultural sector. The ULRP has proposed a new crop pattern for the Miyandoab Plain (Fig. 3), aimed at reducing agricultural water consumption and increasing agricultural profits (Ministry of Energy of Iran, 2016). The proposed crop pattern is the output of a Multi-Objective Decision Making (MODM) model in which economic and environmental goals are considered. This model seeks to increase agricultural income, reduce cultivation costs, maintain market share, and increase environmental flow to Lake Urmia. The constraints considered in this modeling include the following:

- Reducing the area of orchards is costly. Moreover, reducing the area of orchards leads to an increase in unemployment with important social consequences. Therefore, in the proposed crop pattern, the area and pattern of orchards remain unchanged.
- The maximum irrigation demand of the proposed crop pattern is equal to the irrigation demand in the current crop pattern.
- The minimum agricultural profit for the proposed crop pattern is equal to agricultural profit for the current crop pattern.
- Wheat is a staple crop to guarantee food security and is widely cultivated in the Miyandoab Plain. Moreover, wheat has a relatively low water demand (Table S2). The area occupied by wheat was therefore not changed and remains at 55%.
- Sugar beet, tomato, and alfalfa have relatively high water demands (Table S2). In the proposed crop pattern, the areas of these crops were decreased to an extent that does not jeopardize economic activities that depend on these crops, i.e. sugar processing factories, tomato paste factories, and livestock.
- Finally, the proposed crop pattern introduces new low water demand crops such as rapeseed, saffron, and sorghum (Table S2). Saffron and sorghum are high-value crops with a large water productivity (Table S3).

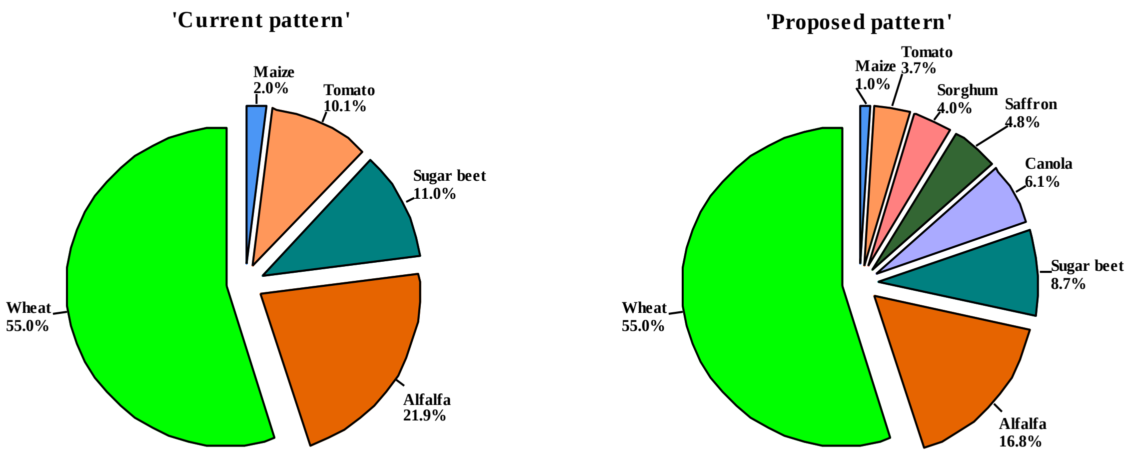

Fig. 3: Current and proposed crop patterns in the Miyandoab Plain (Ministry of Energy of Iran, 2016)

3. Integrated SW-GW Simulation-Optimization Model

In this study, an integrated SW-GW SO model was developed to evaluate different management scenarios in the Miyandoab Plain that achieve sustainable agricultural production without compromising environmental flows to Lake Urmia. An outline of the SO model is shown in Fig. 4. This figure shows how the simulation model interacts with the optimization model. The simulation component consists of three modules: (1) a *hydrologic module* for computing SW-GW flows and storages, (2) an *agronomic module* for computing crop yields, and (3) an *economic module* for computing agricultural profits. The optimization model consists of two conflicting objective functions: *Agricultural index* and *Environmental index*. We used multi-objective optimization based on the Multi-Objective Particle Swarm Optimization (MOPSO) algorithm (Coello et al., 2004) to yield entire Pareto sets of water management strategies that trade off between conflicting objective functions. The SO modeling steps are as follows: The optimization model creates a new population of particles, where each particle represents a set of decision variables for the period 1984-2013. The period 1984-2013 is divided into three hydrological droughts period based on Table 1, and decision variables consist of *crop acreage* (A), the *threshold relative soil water content that triggers irrigation* (Z_{int}), and the *ratio of minimum flow requirement* (MFR) for each hydrological drought conditions. Each particle (i.e., set of decision variables for three hydrological droughts periods) provides input to the simulation model. After that, the hydrologic module in the simulation model runs once and for the entire simulation period (1984-2013) on a monthly time scale. Monthly *actual crop evapotranspiration* (ET_{act}) and *potential crop evapotranspiration* (ET_p) are outputs of the hydrologic module, and they are imported to the agronomic module. Moreover, monthly *downstream river discharge* (inflow into Urmia lake, Q_{out}) and monthly *upstream river discharge* (Q_{in}) are other outputs of the hydrologic module, and they are sent to the optimization model for calculating the environmental index. The agronomic module simulates *actual crop yield* (Y_a) for each crop in each water year and this result is sent to the Economic module to calculate net *agricultural profit* (B). The net agricultural profit is sent to the optimization model to calculate the agricultural index. The process is repeated for each particle in the current population. Finally, non-dominated particles in the population are saved and added to the Pareto set. If the stopping criterion of the optimization model is not reached, a new population of particles is generated by the optimization algorithm, and the entire procedure is repeated. Therefore, the optimization component runs the simulation modules to determine values for the *decision variables* that maximize the *objective functions*, subject to a set of physical *constraints*. In the following sections, we discuss the various parts of the SO model in more detail.

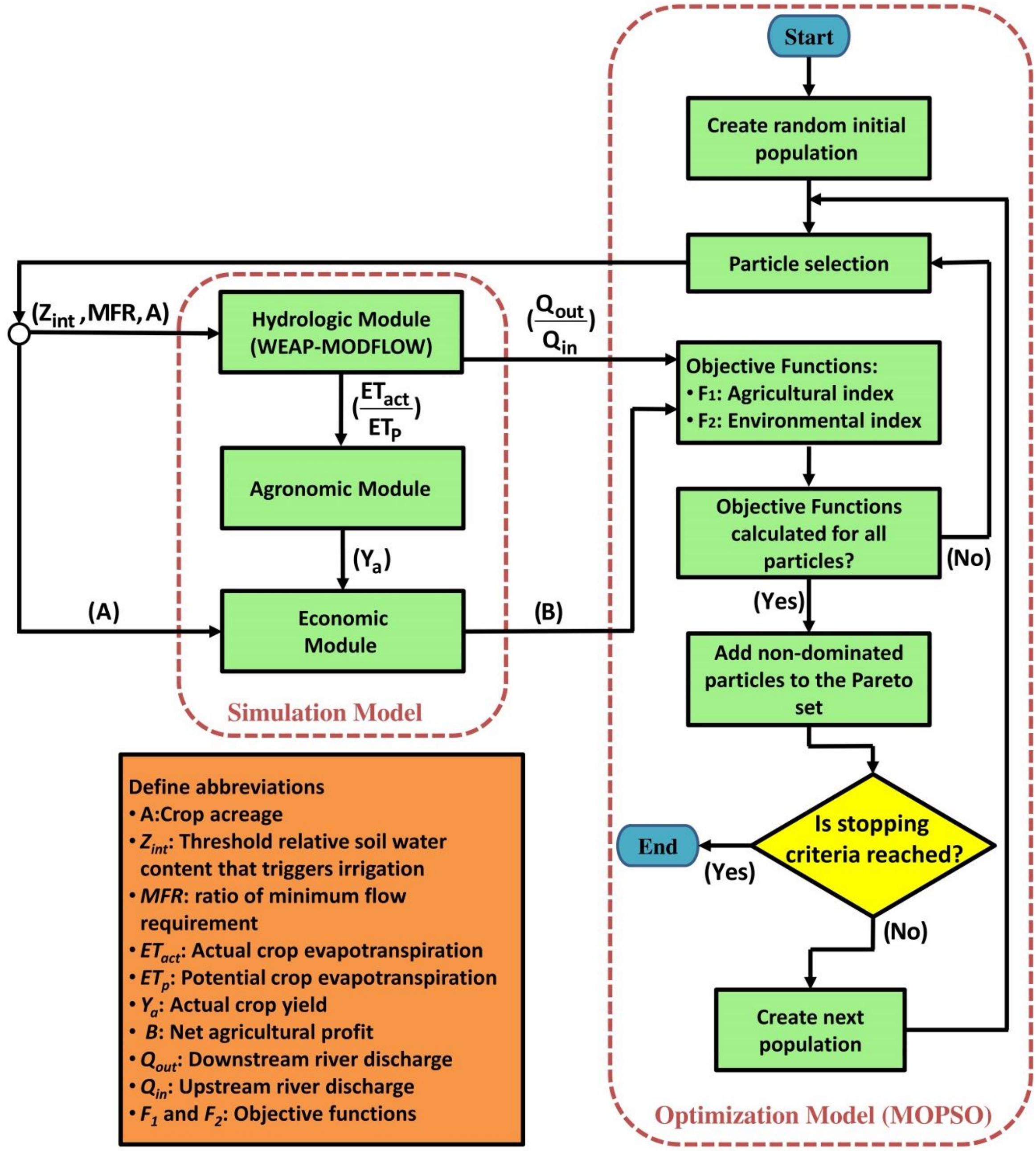

Fig. 4: Outline of the integrated SW-GW Simulation-Optimization model. Each particle in the optimization algorithm represents a set of decision variables.

3.1. Hydrologic Module

The hydrologic module is based on the integrated SW-GW model described in Dehghanipour et al. (2019), who developed a WEAP-MODFLOW model for the Miyandoab Plain. The hydrologic module consists of three interacting spatially distributed water balance components: 1) the crop root zone, 2) the SW system (rivers, surface reservoirs, and irrigation and drainage canals), and 3) the underlying aquifer (Dehghanipour et al., 2019). Fig. 5 shows a schematic diagram of interacting control volumes for all components of the hydrologic module. The monthly water balance is applied to each of the components as follows:

$$\frac{\Delta S}{\Delta t} = \sum Q_i - \sum Q_o \qquad (1)$$

where ΔS is change in water storage (L^3), $\sum Q_i$ is total input (L^3/T) and $\sum Q_o$ is total output (L^3/T). Table 2 summarizes the water balance equation for each physical component and its variables. The hydrologic module was implemented using a dynamic coupling between WEAP and MODFLOW (Harbaugh, 2005; Purkey et al., 2009; Sieber and Purkey, 2015). More details about variables, equations, and implementation of the hydrologic module are presented in Dehghanipour et al. (2019), who showed that the model successfully mimics historically observed river discharge and groundwater levels.

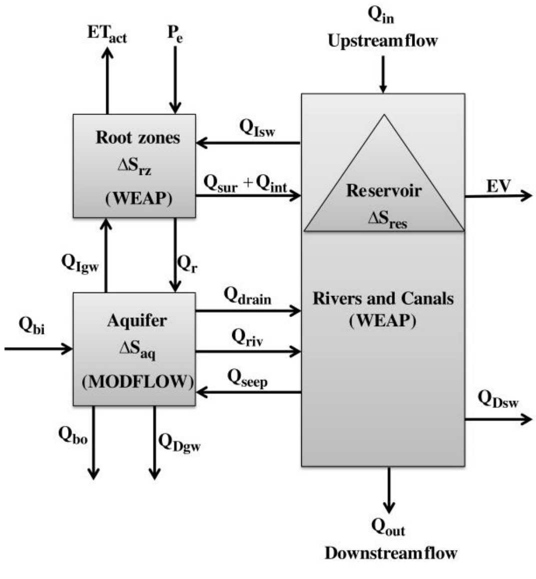

Fig. 5: Schematic diagram of the coupled SW-GW flow model. Variables are defined in Table 2. Each model component is spatially discretized into interacting control volumes for which monthly water balances are formulated (Dehghanipour et al., 2019).

Table 2: Monthly water balance variables and equations for spatially distributed model components shown in Fig. 5.

Variable	Unit	Equation or data source
Storage change in the root zone of each agricultural zone	**L^3/T**	$\frac{\Delta S_{rz}}{\Delta t} = nZ_r A_{rz} \frac{\Delta z}{\Delta t} = Q_{Isw} + Q_{Igw} + P_e A_{rz} - ET_{act} A_{rz} - Q_{sur} - Q_{\text{int}} - Q_r$
Storage change in each aquifer grid cell	**L^3/T**	$\frac{\Delta S_{aq}}{\Delta t} = \text{A}_{\text{aq}}\ \text{S}_{\text{y}}\ \Delta\text{h} = Q_r + Q_{seep} + Q_{bi} - Q_{Igw} - Q_{Dgw} - Q_{riv} - Q_{drain} - Q_{bo}$
Storage change in Bukan reservoir	**L^3/T**	$\frac{\Delta S_{res}}{\Delta t} = Q_{in} - R + \text{A}_{\text{res}}\text{P}_{\text{res}} - \text{A}_{\text{res}}\text{EV}$
Downstream river discharge	**L^3/T**	$Q_{out} = Q_{in} - Q_{Isw} - Q_{Dsw} - Q_{seep} + Q_{riv} + Q_{sur} + Q_{\text{int}} + Q_{drain}$
SW extraction for irrigation	**L^3/T**	Q_{Isw}
GW extraction for irrigation	**L^3/T**	Q_{Igw}
Effective precipitation	**L/T**	P_e
Irrigated area for each crop in each zone	**L^2**	A_{rz}
Actual evapotranspiration	**L/T**	ET_{act}
Surface runoff	**L^3/T**	Q_{sur}
Interflow	**L^3/T**	Q_{int}
GW recharge	**L^3/T**	Q_r
Seepage from river	**L^3/T**	Q_{seep}
Lateral GW flows	**L^3/T**	Q_{bi}, Q_{bo}
GW extraction for drinking	**L^3/T**	Q_{Dgw}
GW discharge to river	**L^3/T**	Q_{riv}
GW discharge to drain	**L^3/T**	Q_{drain}
Grid cell area of aquifer	**L^2**	$A_{aq} = (500\ \text{m})^2$
Upstream river discharge	**L^3/T**	Q_{in}
Downstream river discharge	**L^3/T**	Q_{out}
Downstream release from Bukan reservoir	**L^3/T**	R
Precipitation rate on Bukan reservoir	**L/T**	P_{res}
Bukan reservoir surface area	**L^2**	A_{res}
Evaporation rate from Bukan reservoir	**L/T**	EV
SW extraction for drinking water	**L^3/T**	Q_{Dsw}
Relative soil water content	**-**	z
Rooting depth	**L**	Z_r
hydraulic head (GW level)	**L**	h
Specific yield	**-**	S_y
Porosity	**-**	n

3.2. Agronomic Module

The agronomic module quantifies the impact of deficit irrigation on actual crop yield. It is important to account for changes in crop drought sensitivity throughout the growing season (Srinivasa Prasad et al., 2006). Therefore, the agronomic module uses growth stage specific crop production functions that relate relative evapotranspiration rate (ET_{act}/ET_p) to relative crop yield (Y_a/Y_m). Raes et al. (2005) summarized various ways of modeling the relation between relative crop ET and relative crop yield. Based on the available methods, Eq. 2 was selected because this method accounts for changes in the relation and effects of deficit irrigation at different crop growth stages, and is appropriate for the monthly time-scale of our model.

$$\frac{Y_a}{Y_m} = \prod_{i=1}^{N} (1 - k_{y,i}(1 - \frac{ET_{act,i}}{ET_{p,i}})) \qquad (2)$$

where Y_a and Y_m are actual and potential crop yield (kg/ha) (Table S3), N is total number of crop growth stages (N=4 for wheat, maize, tomato, canola, and sorghum and N=1 for sugar beet, alfalfa, and saffron) (see Fig. S1), $k_{y,i}$ is yield response factor for crop growth stage i (see Fig. S1), $ET_{act,i}$ is actual crop evapotranspiration for crop growth stage i, and $ET_{p,i}$ is potential crop evapotranspiration for crop growth stage *i*. Actual and potential crop evapotranspiration are calculated in the hydrologic module using the following equations:

$$ET_p = k_c(PET) \quad (3)$$

$$ET_{act} = ET_p\left(\frac{5z - 2z^2}{3}\right) \quad (4)$$

where *PET* is reference evapotranspiration based on Penman-Monteith (Allen et al., 1998), k_c is growth stage specific crop coefficient (Table S2), and *z* is relative soil water content (Table 2). Relative soil water content (*z*) is equal to the pore volume fraction filled with water. Values of *z* can range from 0 (dry) to 1 (saturated). The value of *z* in this equation is simulated by the hydrologic module as detailed in Dehghanipour et al. (2019). Eqs. (4) and (2) show that crop yield is directly related to relative soil water content *z*. Therefore, deficit irrigation reduces relative soil water content, which reduces actual crop evapotranspiration and consequently crop production.

3.3. Economic Module

The economic module calculates the net profit of crop production using the following equation:

$$Profit = \sum_u \sum_{cr} A_{u,cr}(Ya_{u,cr}P_{cr} - C_{cr}) - \sum_u DC_u \quad (5)$$

where *u* is the number of agricultural zones (i.e. 21), *cr* is a crop index (going from 1 to 5 or 8 for the current and proposed crop pattern, respectively), $A_{u,cr}$ is crop acreage for crop *cr* in agricultural zone *u* [ha], $Ya_{u,cr}$ is actual crop yield for crop *cr* in agricultural zone *u* [Kg/ha], P_{cr} is price for crop *cr* [USD/Kg], C_{cr} is production cost for crop *cr* excluding maintenance and water delivery costs [USD/ha], and DC_u is maintenance and water delivery costs in agricultural zone *u* [USD]. The actual crop yield is calculated in the agronomic module using Eq. (2). Crop prices and production costs are specified as input parameters to the model (Table S3). Maintenance and water delivery costs are equal to 3% of total gross profit ($\sum_u \sum_{cr} A_{u,cr}(Ya_{u,cr}P_{cr})$), which farmers pay to the Ministry of Energy of Iran.

3.4. Objective Functions

We formulate an optimization problem with two objective functions, i.e. an agricultural index (F_1) quantifying net agricultural profit in the Miyandoab Plain, and an environmental index (F_2) quantifying the degree to which environmental flow requirements to Lake Urmia are met. There is an inherent trade-off between these two objectives, since maximizing profit (F_1) will tend to withdraw more surface water for irrigation, leading to decreased environmental flow (F_2) toward downstream Lake Urmia (Fig. 1).

Two versions of the agricultural index are considered, one focusing on long-term economic profit (economic agricultural index, F_1), and the other focusing on long-term sustainability (sustainable agricultural index, F_1^*). The economic agricultural index is based on long-term net agricultural profit:

$$F_1: Economic\ agricultural\ index = \frac{1}{n}\sum_y \left(\frac{Profit_y}{Profit_{Historical}}\right) \quad (6)$$

where *n* is the number of years simulated (=30), *y* represents a year in the simulation period (1984-2013), $Profit_y$ is net profit in year *y*, and $Profit_{Historical}$ is the historical average net annual profit over the period 1984-2013. $Profit_y$ is calculated by the Economic module. We did not have statistical data for the time series of historical profit and used the simulation model to calculate historical profit. We used available statistical data (for crop acreage, crop pattern, groundwater pumping, and irrigation method) and consider some constraints (for irrigation canals, groundwater pumping, and Bukan reservoir) in the simulation model for calculating the time series of historical profit.

Including historical profits in the objective function provides a useful benchmark: a value equal to 1 for the economic agricultural index indicates a scenario, in which long-term agricultural profits are similar to the historical situation, whereas values greater (smaller) than 1 indicate greater (smaller) profits compared to the historical situation. This objective function prefers values for the decision variables that maximize long-term average agricultural profit without consideration for the inter-annual fluctuations in agricultural profit. For instance, very low profits during droughts are tolerated, as long as this is compensated by high profits during wet periods.

However, such extreme inter-annual variations in profit may not be warranted, and more stable incomes and profits may be preferred. Therefore, an alternative objective function uses a sustainable agricultural index, based on a weighted combination of three sustainability indices (Cai et al., 2002; Schoups et al. 2006):

$$F_1^*: Sustainable\ agricultural\ index = W_1 \frac{REL}{REL_{Historical}} + W_2 \frac{RES}{RES_{Historical}} + W_3 \frac{IVUL}{IVUL_{Historical}} \quad (7)$$

where W_1, W_2, W_3 are three weights, *REL* is net agricultural profit reliability, *RES* is net agricultural profit resiliency, and *IVUL* is net agricultural profit invulnerability. These variables are calculated with the following equations:

$$REL = \frac{1}{n}\sum_y \frac{Profit_y}{Profit_{Historical}} \quad (8)$$

$$RES = 1 - \frac{nfail}{n} \quad (9)$$

$$IVUL = Min\left\{\frac{Profit_y}{Profit_{Historical}}\right\} \quad (10)$$

where *nfail* is the number of successive years that net agricultural profit is smaller than 90% of $Profit_{Historical}$. The *REL* index in the objective function is similar to Eq. (6) and maximizes long-term agricultural profit. This term is driven by agricultural profits in non-drought (HD1) years (Table 1), when there is enough water to meet maximum agricultural water demand. The *RES* index in the objective function prevents extended periods of lower than (90% of) average agricultural profits. This may happen during droughts (successive HD2 and HD3 years, Table 1), when decreased water supply limits agricultural production. We assume 10% as risk threshold, because a reduction in agricultural profit up to

10% has no significant impact on sustainable agricultural profit. Finally, the *IVUL* index prefers decision variables that maximize the smallest agricultural profits over all *n* years. Smallest profit is expected during the most extreme drought conditions, in this case study this corresponds to moderate drought years (HD3, Table 1), since more extreme drought conditions are not encountered in the historical time series. Therefore the *IVUL* index controls the value of agricultural profits during the HD3 period, when there is severe competition between agricultural and environmental water demands. Hence, via the weighted combination of *REL*, *RES*, *IVUL*, the sustainable agricultural index in Eq. (7) considers agricultural profit in each drought period. To prevent significant reductions in agricultural profits, emphasis is placed here on the *IVUL* index, resulting in values for the weights W_1, W_2, *and* $W3$ of 0.25, 0.25, and 0.5, respectively. The environmental objective function is expressed as an environmental index given by the following equation:

$$F_2 : Environmental\ \ index = \frac{1}{n}\sum_{y}\left(\frac{POI_y \times Penalty\ term_y}{POI_{Historical}}\right) \qquad (11)$$

where *POI* is the fraction of the total of all upstream flow into Miyandoab Plain in year *y* that flows to Urmia lake, and is calculated by the following equation:

$$POI_y = \frac{\sum (Q_{out})_y}{\sum (Q_{in})_y} \qquad (12)$$

where summation in the numerator gives total downstream discharge in all rivers that flow out of the Miyandoab Plain and into Lake Urmia, and summation in the denominator gives total upstream discharge in all rivers that flow into Miyandoab Plain. Downstream river discharge is calculated with the hydrologic module. Quantity $Penaltyterm_y$ in Eq. (11) is a fraction between 0 and 1 that penalizes failure to meet minimum environmental flow requirements. It is calculated with the following equation:

$$Penalty\ \ term_y = \begin{cases} 1 & (Q_{out,zar})_y \ge (LD_{zar})_y \\ \dfrac{(Q_{out,zar})_y}{(LD_{zar})_y} & (Q_{out,zar})_y < (LD_{zar})_y \end{cases} \qquad (13)$$

where $(Q_{out,zar})_y$ is downstream discharge to Urmia lake of the Zarrineh Rood river in year *y*, and $(LD_{zar})_y$ is the minimum environmental flow requirement to Urmia lake from Zarrineh Rood in year *y*. Downstream discharge $(Q_{out,zar})_y$ depends on water releases from Bukan reservoir and is calculated with the hydrologic module, whereas $(LD_{zar})_y$ is treated as a decision variable, as discussed in the next section.

Summarizing, we consider two sets of objective functions: strategy I simultaneously maximizes the economic agricultural index F_1 (Eq. 6) and the environmental index F_2 (Eq. 11), while strategy II simultaneously maximizes the sustainable agricultural index F_1^* (Eq. 7) and the environmental index F_2 (Eq. 11). These multi-objective optimization problems are solved using the Multi-Objective Particle Swarm Optimization (MOPSO) algorithm, which results in quantification of the trade-off Pareto front between the two conflicting objective functions (Coello et al., 2004). More details about MOPSO are presented in Dehghanipour et al. (2019).

3.5. Decision Variables

The decision variables for strategies I and II and their lower and upper bounds are listed in Table 3. The decision variables include (1) total crop acreage, (2) threshold relative soil water content to trigger irrigation ("intervention point" z_{int} in Eq. 15), and (3) fraction of inflow to Bukan reservoir allocated for environmental flow. The optimization of complex water resources systems often becomes computationally intractable when solving optimization problems with large numbers of decision variables (Loucks and van Beek, 2005). In this study, to reduce the number of decision variables, we group decision variables by hydrologic drought period based on the SDI. According to Table 1, by using the SDI, the historical period of 30 years (1984-2013) can be divided into periods of non-drought, mild drought, and moderate drought, thus reducing the number of decision variables by a factor of 10 (from 30 years to 3 drought periods).

Total crop acreage directly affects agricultural profit given crop prices and production costs, and it directly affects water consumption in Miyandoab Plain and inflow to Urmia Lake. Treating total crop acreage as a decision variable permits flexibility in dealing with hydrologic drought conditions and agricultural demand. In strategy I, the lower bound for total crop acreage was 0 and the upper bound was set as the total irrigable area, based on studies of the Ministry of Energy of Iran (2016). Moreover, in strategy I we consider three separate decision variables for total crop acreage, one for each drought period (HD1, HD2, and HD3). In strategy II on the other hand, focus is on sustainability of agricultural profits. In that case, the lower bound for total crop acreage was set equal to the current irrigated area. Moreover, to avoid large fluctuations in acreage, we use one decision variable for total crop acreage for all drought periods.

Total crop acreage is distributed over agricultural zones by assuming that each agricultural zone has the same crop pattern:

$$A_{y,u,cr} = A_y \frac{MaxA_u}{\sum_u MaxA_u} \alpha_{cr} \qquad (14)$$

where $A_{y,u,cr}$ is the area of crop cr in agricultural zone u in year y, A_y is total crop acreage in year y, $MaxA_u$ is the irrigable area of agricultural zone u, and α_{cr} is contribution of crop cr in the crop pattern (see Fig. 3). Our analysis considers both crop patterns in Fig. 3. The advantage of using equation (14) is that it ensures spatial equity among agricultural zones in terms of crop production and opportunity for agricultural profit. Another advantage is that it further reduces the number of decision variables (Schoups et al., 2006).

Irrigation demand is a function of relative soil water content so that irrigation begins when relative soil water content drops below a specified threshold or intervention value, z_{int}, and irrigation continues until soil water content reaches a specified target value, z_{tar}. Therefore, irrigation demand, namely the sum of SW and GW withdrawal ($Q_{Isw}+Q_{Igw}$), is calculated as follows:

$$Q_{Isw} + Q_{Igw} = nZ_r A(z_{tar} - z_{\text{int}}) \quad (15)$$

where n is porosity and Z_r is rooting depth (Table 2). Since basin irrigation is used in the Miyandoab Plain, the value of z_{tar} is set equal to 1. Threshold or intervention point z_{int} is treated as a decision variable; it directly affects the level of deficit irrigation and thus agricultural water use, water diversion, and profit. For instance, lower values for z_{int} reduce crop yield and water demand (via Eqs. 2 and 4), and make more water available for environmental flows. As shown in Fig. S1, the FAO considers four values of yield response factor (k_y) for four growth stages of wheat, maize, tomato, canola, and sorghum, and one value of k_y for the entire growing season of sugar beet, alfalfa, and saffron. Therefore, we consider four distinct intervention points each for wheat, maize, tomato, canola, and sorghum, and one intervention point each for sugar beet, alfalfa, and saffron. The advantage of using these growth-stage specific decision variables is that it permits flexibility in deficit irrigation for dealing with water shortage and changes in the timing of irrigation according to the growth stage of each crop. The upper bound of each z_{int} decision variable was set equal to 60%, which for the loamy soils in the area corresponds to field capacity (Schroeder et al., 1994), while the lower bound of each z_{int} decision variable was set to 30%, which is between wilting point (22%) and field capacity (60%).

The final decision variable relates to environmental flow releases to Urmia Lake from Bukan reservoir located on the Zarrineh Rood river. Specifically, we use the fraction *MFR* of inflow into Bukan reservoir that is released as environmental flow as a decision variable:

$$MFR = \frac{(LD_{zar})_{y,m}}{(Q_{in,zar})_{y,m}} \quad (16)$$

where $(LD_{zar})_{y,m}$ is the minimum environmental flow requirement for Urmia lake from Zarrineh Rood river in year y in month m, and $(Q_{in,zar})_{y,m}$ is the upstream flow of Zarrineh Rood river into Bukan reservoir in year y and month m. Lower and upper bounds of *MFR* are taken as 0.2 and 0.85, respectively (Yasi and Ashori, 2017).

In strategy I, we consider one single decision variable for *MFR* that is constant over the entire period; this choice is expected to reduce large fluctuations in environmental flow to Urmia Lake, and thus result in a temporally stable environmental index. As mentioned above, three decision variables are considered for total crop acreage in strategy I. This degree of freedom allows total crop acreage to be modified to meet minimum environmental flow requirements. In contrast, in strategy II, we consider three decision variables for *MFR* for each drought period (HD1, HD2, and HD3), but one single decision variable for total crop acreage for the entire period. This promotes temporal stability in agricultural profits, with additional flexibility in *MFR* to meet agricultural and environmental water demand.

Finally, an important constraint relates to the monthly timing of agricultural and environmental water demand. Fig. 6 shows monthly time-averaged inflow to Bukan reservoir (upstream flow of Zarrineh Rood river) together with monthly potential evapotranspiration (ET_p). Following Eq. 16, environmental flow is allocated proportional to inflow into Bukan reservoir, which mostly occurs from early winter to mid-spring. Therefore, the value of *MFR* has the most significant effect on water storage in Bukan reservoir from early winter to mid-spring, because by increasing *MFR*, more water will be allocated to the lake in this period and less water storage will remain in the reservoir to meet agricultural demand in the spring and summer. On the other hand, the total crop acreage and deficit irrigation (intervention point) decision variables have the most significant effect on water storage in Bukan reservoir from early spring to end of summer, since these variables play a crucial role in agricultural water consumption.

Table 3: Decision variables for the two sets of objective functions in section 3.4

Strategy	Objective Functions	Decision Variable[a]	Lower Bound	Upper Bound	Units[b]	Number of Variables[c]
I	(F_1, F_2)	A_y	0	76700	ha	np
		$Zint_{y,cr,s}$	30%	60%	-	$\sum_{ncrop} np \times ns_{ncrop}$
		MFR	20%	85%	-	1
II	(F_1*, F_2)	A_y	54200	76700	ha	1
		$Zint_{y,cr,s}$	30%	60%	-	$\sum_{ncrop} np \times ns_{ncrop}$
		MFR	20%	85%	-	np

[a] A_y: Total crop acreage in year *y*, $Zint_{y,cr,s}$: threshold soil moisture content in year *y* for crop *cr* in growth stage *s*, MFR: Minimum flow requirement to Urmia lake from the Zarrineh Rood river

[b] ha=hectare, 10^4 m^2

[c] *np* is number of distinct hydrologic drought periods (=3), *ncrop* is number of crops (5 in current crop pattern and 8 in proposed crop pattern), *ns* is number of crop growth stages (4 for wheat, maize, tomato, canola, and sorghum, and 1 for sugar beet, alfalfa, and saffron).

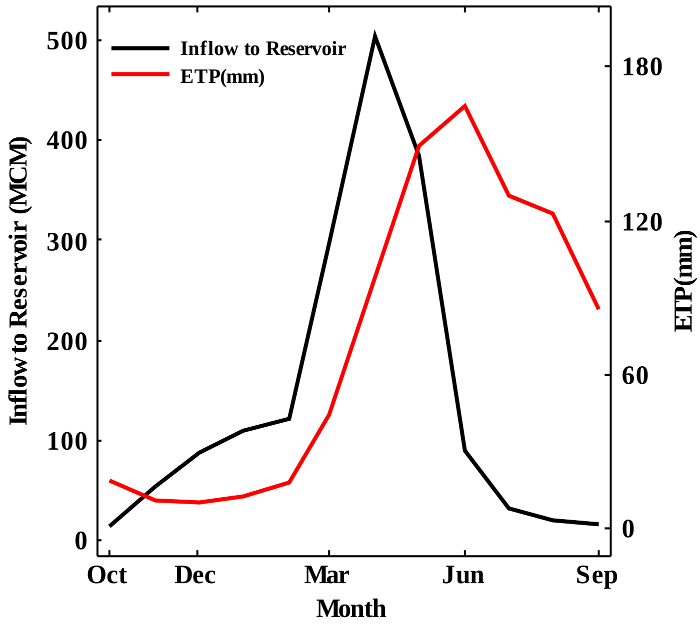

Fig. 6: Monthly time-averaged inflow to Bukan reservoir (i.e, upstream discharge of Zarrineh Rood river) (MCM) and potential evapotranspiration (ETp) (mm) in Miyandoab Plain

3.6. Variable Constraints

Three sets of variable constraints are used to ensure realism of the optimization results. The first set of constraints limits GW pumping in each agriculture zone to the monthly GW pumping capacity of the zone:

$$Pump_{m,u} \leq PumpCap_{u} \qquad (17)$$

where $Pump_{m,u}$ is GW extraction in agricultural zone u in month m [L^3/T], and $PumpCap_u$ is GW pumping capacity in agricultural zone u [L^3/T]. In this study, the sum of the historically measured maximum monthly pumping rate of wells in each agricultural zone was considered as the monthly pumping capacity for each agriculture zone. This constraint ensures that the optimal solution reflects realistic maximum pumping rates.

SW diversions from the Zarrineh Rood river are conveyed to the primary irrigation canals. Each irrigation canal has a diversion capacity based on its dimensions.

$$Q_{m,c} \leq MaxQ_{c} \qquad (18)$$

where $Q_{m,c}$ is SW diversion to canal c in month m [L^3/T], and $MaxQ_{m,c}$ is diversion capacity of canal c [L^3/T]. This constraint ensures that total monthly SW diversions do not exceed canal conveyance capacities.

Finally, constraints are placed on monthly water storage $S_{y,t}$ in Bukan reservoir:

$$S_{dead} \leq S_{y,t} \leq S_{max} \qquad (19)$$

where S_{dead} is dead storage volume of the reservoir and S_{max} is maximum volume of the reservoir. These constraints prevent water releases from dead storage, and allow for releases larger than total water demand (sum of agricultural, urban, and environmental water demand) when the reservoir is full and overtopping occurs.

4. Results and discussion

4.1. Water management scenarios for current and proposed crop patterns in strategy I

The Pareto fronts for current and proposed crop patterns in strategy I, i.e., the set of non-dominated simulations that were obtained with the integrated SO water management model, are presented in Figure 7.a. In Fig. 7.a, objective function 2 (Environmental index) is plotted against objective function 1 (Economic agricultural index), and dark and blue nodes indicate the Pareto fronts for current and proposed crop patterns, respectively. The Pareto front consists of many solutions and presents potential compromises between contradicting objectives. In this study, six scenarios that indicate specific optimal solutions on the Pareto fronts for strategy I were selected for detailed analysis. These scenarios include scenarios 1 to 6, as shown by the yellow nodes in Fig. 7.a. Furthermore, the orange node represents values for the objective functions corresponding to historical water management, which serves as a benchmark.

Scenarios 1 and 4 represent environmental scenarios characterized by an increase in Environmental index without a change in Economic agricultural index compared to historical conditions. Likewise, scenarios 3 and 6 are economic scenarios with an increase in the Economic agricultural index without a change in Environmental index compared to historical conditions. Finally, scenarios 2 and 5 represent win-win situations where both Environmental and Economic agricultural indices are increased compared to historical conditions.

In scenario 1, changes in water management (deficit irrigation, changes in crop acreage, and environmental flow requirement) with the current crop pattern make it possible to increase the Environmental index by 9% without decreasing the Economic agricultural index. However, increasing the Environmental index by more than 9% leads to significant reductions in Economic agricultural index. Likewise, changes in water management with the current crop pattern in scenario 3 increase the Economic agricultural index by 14% without decreasing the Environmental index, with further increases in Economic agricultural index requiring significant reductions in the Environmental index.

Similar trade-offs are present in the Pareto front for the proposed crop pattern (Fig. 7a), but at larger values for both objective functions, thereby clearly demonstrating benefits of the proposed crop pattern on both the agricultural economy and the environment. For example, scenario 4 increases the Environmental index by 16% (up from 9% in scenario 1), while scenario 6 increases the Economic agricultural index by 24% (up from 14% in scenario 3).

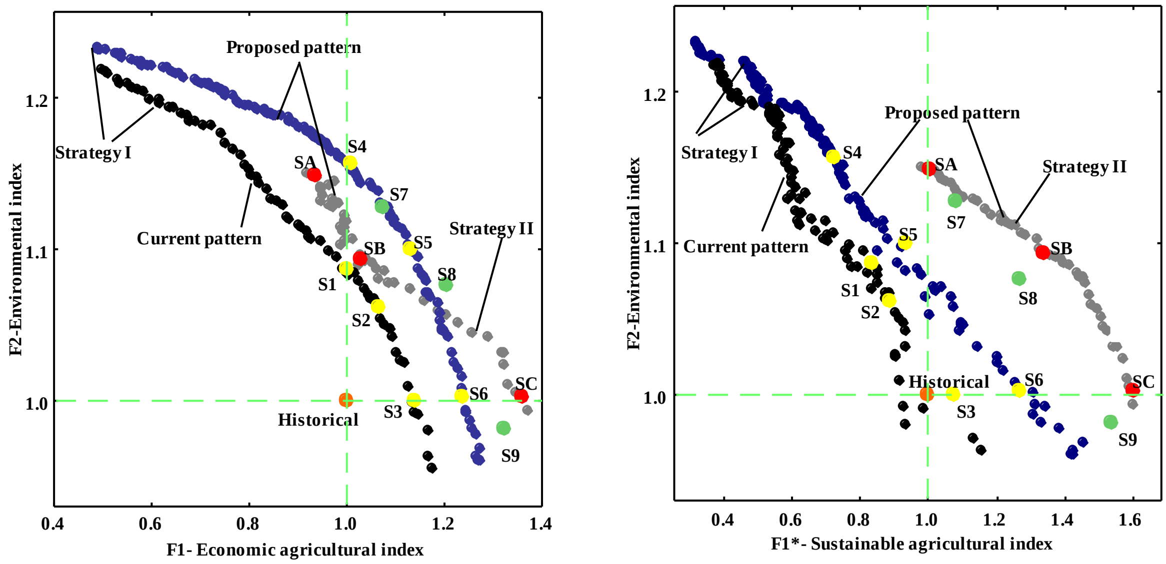

(a) (b)

Fig. 7: Pareto fronts for the multi-objective optimization after 5000 model simulations with the MOPSO algorithm for strategy I and II: (a) Environmental index vs Economic agricultural index, and (b) Environmental index vs Sustainable agricultural index. Black and blue nodes indicate Pareto fronts for current and proposed crop patterns in strategy I (section 4.1), while gray nodes indicate the Pareto front for the proposed crop pattern in strategy II (section 4.3). The orange node represents historical conditions and is used as reference. Selected points on the trade-off curves ("scenarios") are indicated by yellow and red nodes and are discussed in more detail in the text. The green nodes are simulation scenarios showing the effect of increased GW capacity (S4 moves to S7, S5 moves to S8, S6 moves to S9) as discussed in section 4.2.

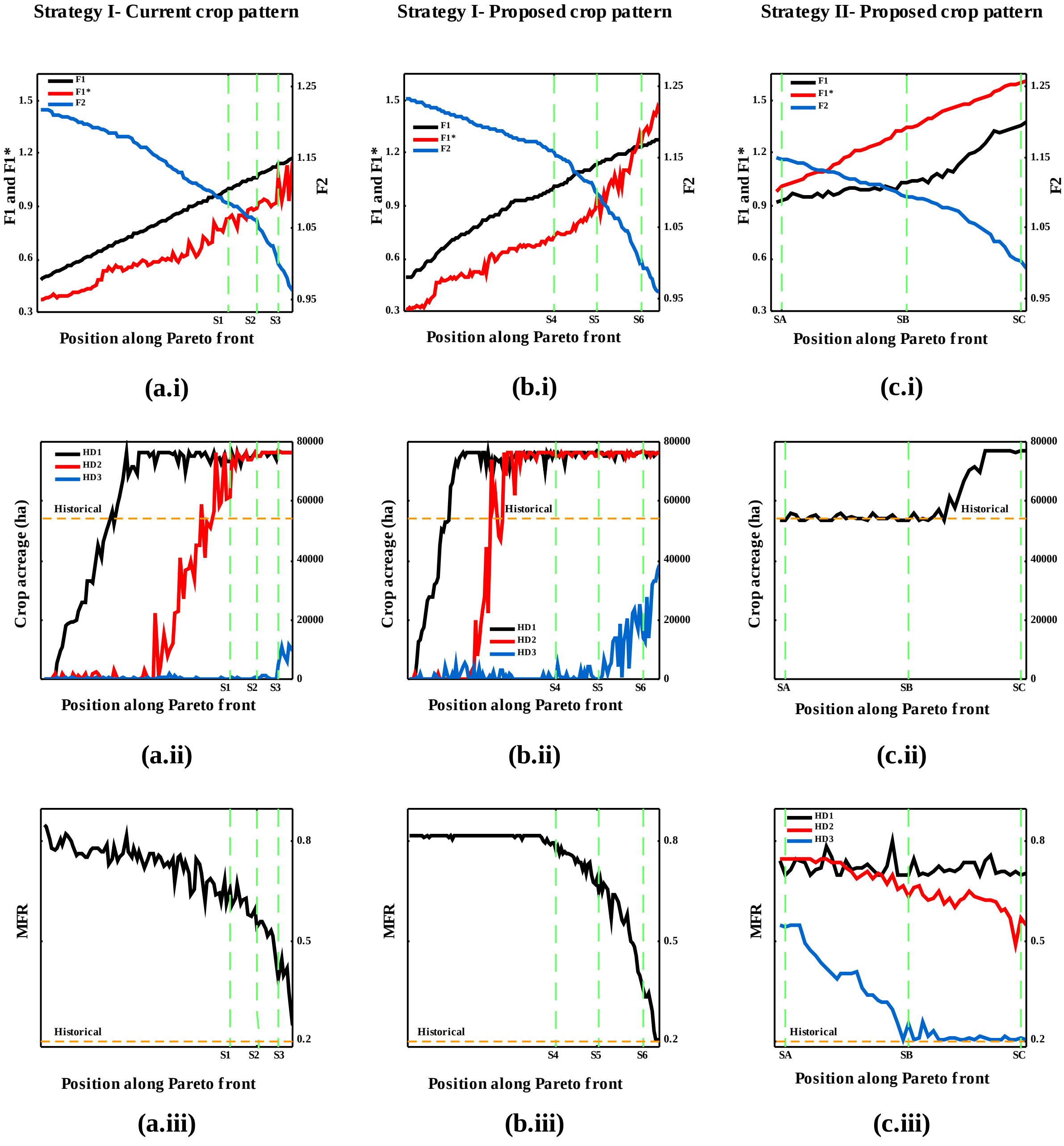

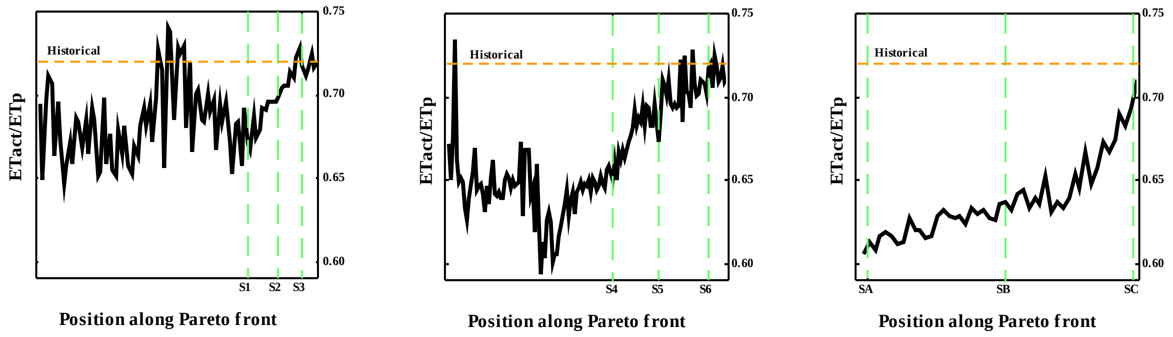

(a.iv) **(b.iv)** **(c.iv)**

Fig. 8: Changes in values for the objective functions and decision variables when moving along the Pareto fronts from left (focus on environment) to right (focus on agriculture). Each column shows a different Pareto front: (a) strategy I with current crop pattern, (b) strategy I with proposed crop pattern, and (c) strategy II with proposed crop pattern. Each row shows a different variable: (i) objective functions, (ii) crop acreage, (iii) minimum environmental flow requirement MFR, and (iv) ratio of actual to potential crop ET (a measure of deficit irrigation). HD1, HD2, HD3 are hydrologic drought conditions defined in Table 1.

Figure 8 provides more detailed insight into how optimal water management changes as one moves along each of the Pareto fronts in Fig. 7. Moving from left to right along each Pareto front changes the focus from the environment to agriculture. In strategy I (columns a and b in Fig. 8), the resulting increase in Economic agricultural index (row i in Fig. 8) is achieved by increasing crop acreage (row ii), decreasing environmental flow requirement (row iii), and decreasing deficit irrigation (row iv).

When moving along the Pareto front, crop acreage in non-drought years (HD1) increases first, followed by an increase in crop acreage in mild-drought years (HD2). Significantly, crop acreage in moderate-drought years (HD3) remains near zero along most of the Pareto front, and only starts to increase on the far-right end of the strategy I Pareto curves, when the environment is all but ignored. This increase is more pronounced with the proposed than with the current crop pattern (compare Fig. 8.a.ii and 8.b.ii), because of the lower water requirements of the proposed crop pattern (Table S4 and Table S5). These results indicate that, even though strategy I results in better water management with benefits for both the environment and agriculture, it does not protect agriculture against short-term effects of moderate to severe droughts. This is also clear in Fig. 7b, where the strategy I Pareto scenarios do not score that well on the Sustainable agricultural index. More sustainable management strategies may therefore be required (see sections 4.2 and 4.3).

Once crop acreages are at their maximum level, further increases in the Economic agricultural index are achieved by reducing environmental flow requirement (Fig. 8.a.iii and 8.b.iii), which reallocates water to agriculture, and reducing deficit irrigation (Figs. 8a.iv, 8.b.iv, and S3). These effects are visible when moving from scenario 1 to scenario 3 (column a in Fig. 8), and similarly when moving from scenario 4 to scenario 6 (column b in Fig. 8).

The dynamics of annual agricultural profit (relative to historical) for six Pareto scenarios are shown in Fig. 9a. In non-drought (HD1) years and pre-2008 mild-drought (HD2) years (1984, 1986, 1989, 1990, 1991, 1997, 2002, 2006, 2007), agricultural profits for all scenarios are equal or higher than historical profits (Fig. 9.a), because of the larger total crop acreages for those years compared to historical ($A_{historical}$=54200 ha).

In post-2008 HD2 years (2009-2013), agricultural profit is less than historical in the environmental scenarios (scenarios 1 and 4) and the win-win scenarios (scenarios 2 and 5). The reason for this is greater water allocation to the environment (larger MFR) in those years compared to historical, resulting in deficit irrigation and crop water stress. Finally, in the moderate-drought (HD3) years (1999-2001, and 2008), all scenarios, with the exception of scenario 6, exhibit a sharp decrease in agricultural profit, due to near-zero crop acreages in those years, with agricultural production limited to orchards. This confirms the lower scores of these scenarios on the Sustainable agricultural index, as already seen in Fig. 7b.

Figure 9.b shows dynamics of annual inflow to Lake Urmia relative to historical conditions. As mentioned before, the *MFR* and crop acreage of the six scenarios in HD1 and HD2 years are higher than historical ($MFR_{historical}$=0.2 and $A_{historical}$=54200 ha), which increases environmental flow requirement and agricultural demand compared to historical conditions. In HD3 years, inflow to Lake Urmia is more stable in the six Pareto scenarios compared to historical. This is in line with lower crop acreages in those years (Fig. 9a), less irrigation water withdrawals, and thus relatively more water available for the environment.

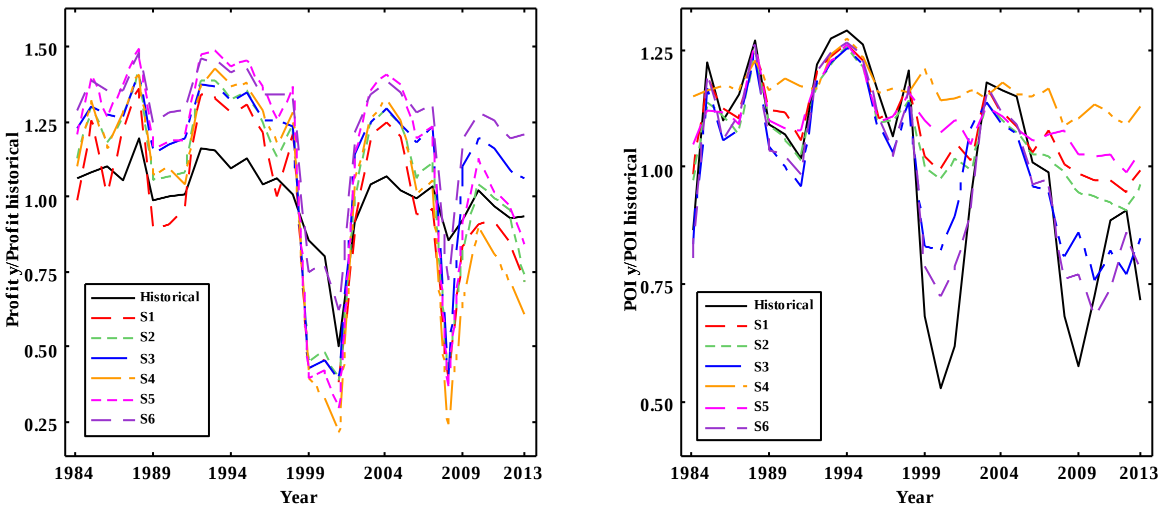

(a) **(b)**

Fig. 9: Time series of (a) annual agricultural profit and (b) inflow to Lake Urmia expressed as POI in Eq. 12 (both relative to average historical conditions) for six Pareto scenarios of strategy I (S1-S3 use the current crop pattern, S4-S6 use the proposed crop pattern).

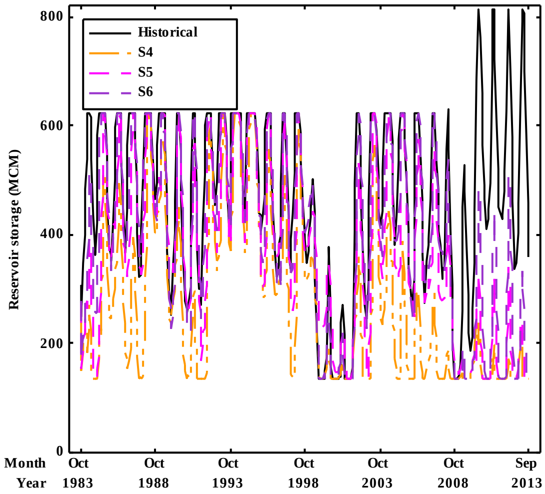

Fig. 10: Time series of monthly Bukan reservoir storage for three Pareto scenarios of strategy I with the proposed crop pattern.

Next, Fig. 10 shows dynamics of water storage in Bukan reservoir. More water is stored in scenarios that focus on irrigation (e.g. S6), due to the delay between reservoir inflow and crop water demand, as shown in Fig. 6. In 2008, dam height and storage capacity of Bukan reservoir was increased from 650 to 808 MCM, as clearly visible in Fig. 10. The purpose of this increase was to ensure sufficient water supply to nearby cities in extreme droughts. Historically, the increased capacity has led to more water being stored in the reservoir after 2008 (Fig. 10), resulting in relatively less water allocation to agriculture and Lake Urmia. All scenarios in Fig. 10 show that storing less and releasing more water leads to greater benefits.

Finally, the water management model also provides insights into the effects of water management on the root-zone water balance in the region (Table S4 and Table S5). As expected, GW pumping, SW withdrawal, and actual crop ET all increase from scenario 1 to 3 (and from scenario 4 to 6), which correspond to increasing Economic agricultural index and decreasing Environmental index. Increases in actual crop ET reflect decreases in deficit irrigation, i.e. more water available for irrigation and less for environmental flow to the lake.

Note that SW withdrawal, GW pumping, and actual crop ET in the proposed-crop-pattern scenarios (4, 5, and 6) are lower than the corresponding current-crop-pattern scenarios (1, 2, and 3), due to the lower water requirements for the proposed crop pattern.

4.2. Increasing GW pumping capacity: a simulation analysis of strategy I scenarios

The previous section illustrated that water management based on strategy I scenarios results in sharp decreases in agricultural profit during droughts (Fig. 9). Even though groundwater is in principle available to deal with such shocks, current pumping capacity limits greater reliance on groundwater during droughts. This section investigates to what extent an increase in GW pumping capacity can improve agricultural sustainability during droughts without compromising GW level stability. To this end, scenarios S4-S6 (proposed crop pattern) are taken as starting point, and are modified into three new scenarios (S7-S9). The modifications are detailed in Table S6, and basically correspond to changing crop acreage and GW pumping capacity in the model during the dry HD3 years: crop acreage is set equal to the historical acreage (about 75% of the maximum area), while GW pumping capacity is doubled.

The model is then run with these new inputs (i.e., a simulation is done, not an optimization), and the resulting values of the objective functions are shown in Fig. 7. We see that scenarios 7, 8, and 9 result in greater values for the Economic agricultural index, but smaller values for the Environmental index, compared to the corresponding scenarios 4, 5, and 6 (Fig. 7a). Furthermore, the effect on the Sustainable agricultural index is significant (Fig. 7b), suggesting greater agricultural sustainability of these new scenarios that use an increased GW pumping capacity. These observations are confirmed by the time-series in Fig. 11, which show increased agricultural profits during droughts, but also decreases in environmental flows to the lake. This indicates that the doubled GW pumping capacity used in these new scenarios is not sufficient to support the targeted crop acreages without reallocating additional surface water from the environment to agriculture.

The effects of increased GW pumping on the water balance and on groundwater levels are shown in Figs. S4 and 12. Drops in groundwater level are most pronounced in scenario 7 (Fig. 12), which, out of the three new scenarios, is characterized by the largest SW allocation to the lake, the smallest SW extraction for irrigation, largest fraction of GW use for irrigation, and the smallest GW recharge (Fig. S4).

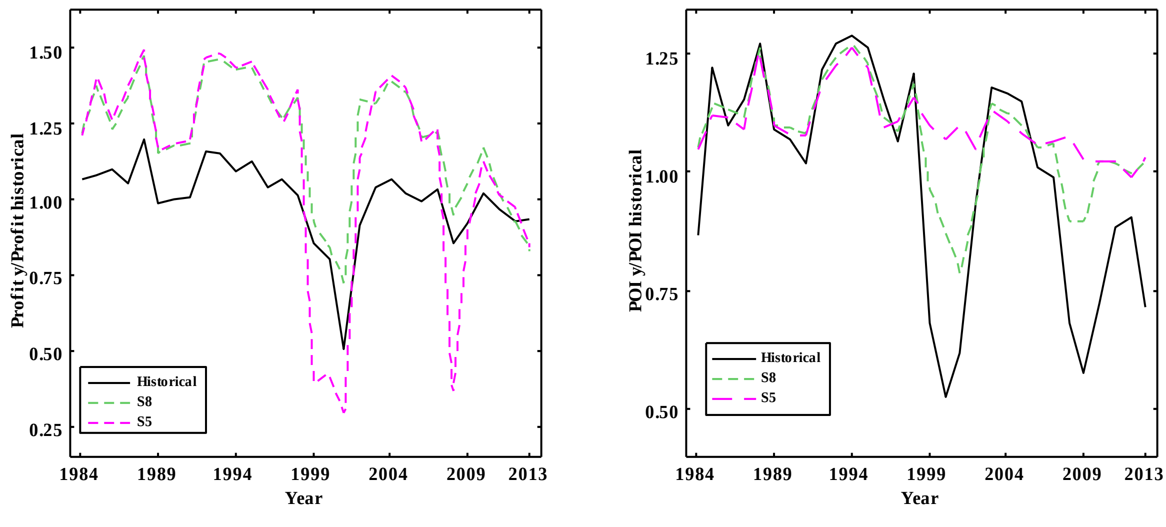

(a) **(b)**

Fig. 11: Time series of (a) annual agricultural profit, and (b) inflow into lake Urmia expressed as POI in Eq. 12, for scenario 5 (original GW pumping capacity) and scenario 8 (doubled GW pumping capacity).

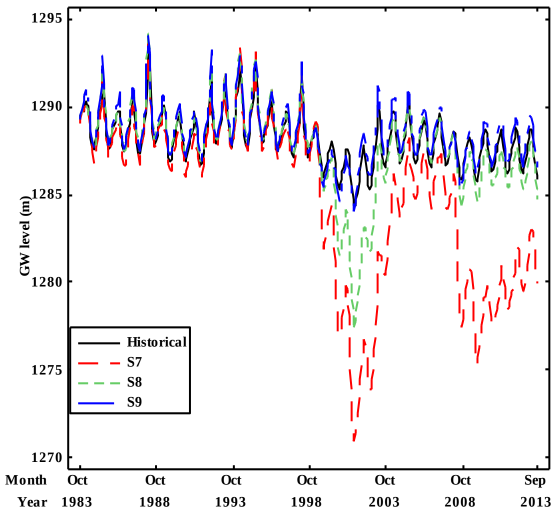

Fig. 12: Time-series of monthly GW level for increased GW pumping capacity scenarios 7 to 9.

4.3. Water management scenarios for proposed crop pattern in strategy II

In addition to simulation as used in section 4.2, sustainable water management options can also be explored by directly optimizing the Sustainable agricultural index. These strategy II results are presented in this section. The resulting Pareto front for proposed crop pattern in strategy II is shown in Fig. 7 with gray nodes. We focus on three specific Pareto scenarios A, B, and C shown in red in Fig. 7. These scenarios show that it is possible to, compared to historical conditions, (1) increase the Environmental index without any decrease in the Sustainable agricultural index (scenario A), (2) increase the Sustainable agricultural index without a change in the Environmental index (scenario C), and (3) increase both the Environmental and Sustainable agricultural index at the same time (scenario B).

The third column in Fig. 8 shows how optimal water management changes along the Pareto front of strategy II. The value of the Sustainable agricultural index increases when moving across the Pareto front from left to right. In the first half of the Pareto front, this increase is achieved, not by increasing crop acreage, which remains constant initially, but by decreasing the environmental flow requirement (*MFR*) during moderate droughts (HD3), which has the effect of reallocating SW from the environment to agriculture. It is only in the second half of the Pareto front that further increases in the Sustainable agricultural index are achieved by increasing crop acreage and decreasing deficit irrigation (Fig. 8.c.iv and Fig. S5).

As shown in Fig. 8.c.iii, the environmental flow requirement (*MFR*) in the HD1 years is constant and close to the maximum level, while *MFR* in the HD2 years decreases only slightly. This indicates that the environmental flow requirement of the lake is met in the HD1 and HD2 years (non- and mild-droughts). Hence, the trade-off in water allocation between the environment and agriculture only really comes into play during moderate droughts (HD3 years), as shown by the decrease in *MFR* during HD3 years in Fig. 8.c.iii: temporarily reducing water allocations to the environment during moderate-droughts benefits agricultural production and sustainability. Such a strategy is illustrated by scenario SB in Fig. 13: sharp decreases in agricultural profit during droughts are prevented at the expense of temporary decreases in environmental flow to the lake. Such a strategy could make sense as long as it results in short-term decreases in lake water level that fully recover during the next non-drought period, thereby avoiding any long-term downward trend in lake water level.

In terms of agricultural profit, there is also a trade-off between maximizing net agricultural profit, as done in strategy I, and preventing significant decreases in profit during droughts. This becomes clear by plotting the Pareto front of strategy II in Fig. 7.a next to the Pareto front of strategy I: the Economic agricultural index for scenarios A and B is less than for scenarios 4 and 5, due to lower crop acreages in the former. However, crop acreage of scenario C is equal (HD1, HD2) or larger (HD3) than crop acreage of scenario 6, making scenario C superior for both Economic and Sustainable agricultural indices. On the other hand, scenario C does not score well on the Environmental index.

Fig. S6 shows the monthly time series of the Bukan storage reservoir for scenarios A, B, and C of strategy II. The maximum storage volumes for all scenarios are less than 650 MCM. As mentioned before, this result indicates that increasing the storage capacity of the reservoir after 2008 does not contribute to higher values for the objective functions. Finally, Fig. S7 shows time series of monthly GW levels, which are similar to historical conditions.

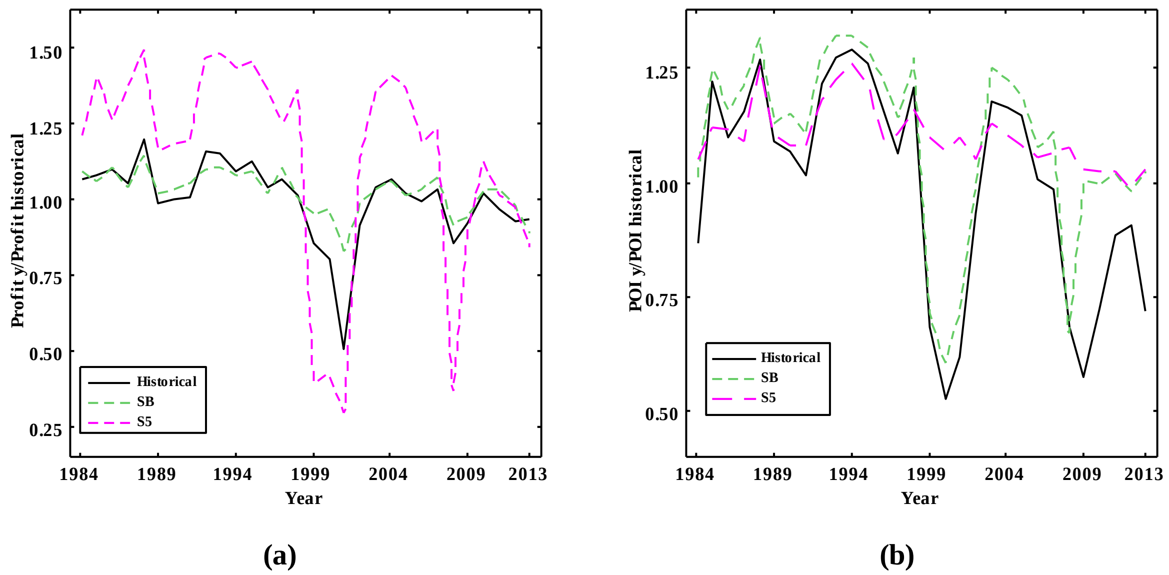

Fig. 13: Time series of (a) annual agricultural profit and, (b) annual inflow to lake Urmia expressed as POI in Eq. 12, for the win-win Pareto scenarios of strategy I (S5) and strategy II (SB).

In this study, we tried to reduce uncertainty in the development of the simulation-optimization model. For instance, all input data come from government agencies in Iran that have established data quality control procedures. Furthermore, we used multi-objective calibration for the hydrologic module. The advantage of multi-objective calibration with both river discharge data and groundwater level data (two independent datasets) is that we can identify any inconsistencies in the model and/or the data. The absence of significant trade-offs in fitting these two observation datasets in the multi-objective calibration of the hydrologic model provides some confidence in the outputs of the hydrological model for the water balance component (Dehghanipour et al., 2019). However, we believe that more research is required to quantify and consider uncertainty in the development of the simulation-optimization model. For example, future climate change , will lead to changes in climatic variables, e.g., temperature, precipitation, snow, and evapotranspiration, that in turn result in changes in river runoff and surface water availability. Therefore, climate change is causing uncertainty in the inflow to reservoirs and related planning (Hakami-Kermani et al., 2020). Consequently, future work will focus on assessing the effects of climate change uncertainty on the planning and management of water resources to meet agricultural water demand in Miyandoab plain and environmental flow requirements of Urmia Lake.

5. Conclusions

The paper has presented and applied a simulation-optimization (SO) approach for identifying water management strategies in irrigated endorheic river basins that ensure sustainability of irrigated agriculture while meeting downstream environmental flow requirements. Our analysis contributes both novel methodology and novel insights into water management in the application case study.

In terms of methodology; first, the issue of estimating minimum environmental flow requirements is tackled by including it as a decision variable in the optimization model, which adds more flexibility compared to existing approaches that either include it as a precomputed constraint or as an objective to be maximized. Second, the hydrologic simulation model in our SO approach includes both SW and GW components in the form of dynamically coupled WEAP and MODFLOW models. As such, the optimization model searches a larger solution space that includes conjunctive use as a potential long-term strategy. Finally, multi-objective optimization is used to yield an entire Pareto set of water management strategies that quantify the trade-off between meeting environmental water demand, quantified by an environmental flow objective function, and meeting agricultural water demand, quantified by either a maximum or sustainable profit objective function.

The methodology was applied to the irrigated Miyandoab Plain, a strategic agricultural region in the semi-arid and endorheic Lake Urmia basin, located in the northwest of Iran. There is direct competition between environmental flow requirements tot sustain water levels of Lake Urmia and upstream irrigation withdrawals in the Miyandoab Plain. A recent drought in the region has further increased this competition and led to decreased flow into and continued shrinking of the lake. Results show that a specific combination of minimum environmental flow requirements, deficit irrigation, and cropping patterns can increase environmental flow to Lake Urmia by up to ~16% compared to historical conditions, without decreasing agricultural profits. An alternative combination of these decision variables increases agricultural profits by up to 24% compared to historical conditions, without decreasing environmental flows to the lake. Multiple trade-off options also exist in between these two extremes that simultaneously increase the environmental and agricultural objectives compared to historical conditions. A disadvantage of strategies that maximize long-term agricultural profit is that they result in significant drops in agricultural profit during droughts. An alternative multi-objective optimization was therefore considered which replaced the agricultural profit-maximizing objective with an objective function that emphasizes sustainability of agricultural profits. This analysis revealed that drops in agricultural profit during droughts can be avoided by increasing agricultural GW pumping capacity and temporarily reducing the lake's minimum environmental flow requirements. This may be an attractive strategy during droughts that are neither too long or too severe, so that resulting declines in groundwater and lake water levels are temporary and fully recover after the drought. Overall, the application highlights the feasibility and flexibility of the proposed approach in identifying a range of potential water management strategies in a complex agricultural endorheic basin like the Lake Urmia basin.

Competing interests

The authors declare no competing interests.

Funding source

This research did not receive any specific grant from funding agencies in the public, commercial, or not-for-profit sectors.

Acknowledgment

We are grateful to the Ministry of Energy of Iran, Urmia Lake Restoration Program (ULRP), and I.R. of Iran Meteorological Organization (IRIMO) for providing the primary data for this research study. We appreciate valuable help from experts of the department of water resources in Yekom Consulting Engineers Company (http://www.yekom.com/).

Reference

Ahmadzadeh, H., Morid, S., Delavar, M., Srinivasan, R., 2016. Using the SWAT model to assess the impacts of changing irrigation from surface to pressurized systems on water productivity and water saving in the Zarrineh Rud catchment. Agric. Water Manag. 175, 15–28. https://doi.org/10.1016/j.agwat.2015.10.026

Allen, R.G., Pereira, L.S., Raes, D., Smith, M., 1998. FAO Irrigation and drainage paper No. 56. Rome: Food and Agriculture Organization of the United Nations.

Anghileri, D., Castelletti, A., Pianosi, F., Soncini-Sessa, R., Weber, E., 2013. Optimizing watershed management by coordinated operation of storing facilities. J. Water Resour. Plan. Manag. 139, 492–500. https://doi.org/10.1061/(ASCE)WR.1943-5452.0000313

Arthington, A.H., Bhaduri, A., Bunn, S.E., Jackson, S.E., Tharme, R.E., Tickner, D., Young, B., Acreman, M., Baker, N., Capon, S., Horne, A.C., Kendy, E., McClain, M.E., Poff, N.L., Richter, B.D., Ward, S., 2018. The Brisbane Declaration and Global Action Agenda on Environmental Flows (2018). Front. Environ. Sci. 6. https://doi.org/10.3389/fenvs.2018.00045

Bai, J., Chen, X., Li, J., Yang, L., Fang, H., 2011. Changes in the area of inland lakes in arid regions of central Asia during the past 30 years. Environ. Monit. Assess. 178, 247–256. https://doi.org/10.1007/s10661-010-1686-y

Bai, J., Chen, X., Yang, L., Fang, H., 2012. Monitoring variations of inland lakes in the arid region of Central Asia. Front. Earth Sci. 6, 147–156. https://doi.org/10.1007/s11707-012-0316-0

Barbier, E.B., Koch, E.W., Silliman, B.R., Hacker, S.D., Wolanski, E., Primavera, J., Granek, E.F., Polasky, S., Aswani, S., Cramer, L.A., Stoms, D.M., 2009. Coastal ecosystem-based management with nonlinear in ecological functions and values. Zhongguo Renkou Ziyuan Yu Huan Jing/ China Popul. Resour. Environ. 19, 125–128. https://doi.org/10.1126/science.1150349

Cai, X., McKinney, D.C., Lasdon, L.S., 2002. A framework for sustainability analysis in water resources management and application to the Syr Darya Basin. Water Resour. Res. 38, 21-1-21–14. https://doi.org/10.1029/2001wr000214

Cai, X., Rosegrant, M.W., 2004. Optional water development strategies for the Yellow River Basin: Balancing agricultural and ecological water demands. Water Resour. Res. 40. https://doi.org/10.1029/2003WR002488

Chunyu, X., Huang, F., Xia, Z., Zhang, D., Chen, X., Xie, Y., 2019. Assessing the Ecological Effects of Water Transport to a Lake in Arid Regions: A Case Study of Qingtu Lake in Shiyang River Basin, Northwest China. Int. J. Environ. Res. Public Health 16, 145. https://doi.org/10.3390/ijerph16010145

Coello, C.A.C., Pulido, G.T., Lechuga, M.S., 2004. Handling Multiple Objectives With Particle Swarm Optimization. IEEE Trans. Evol. Comput. 8, 256–279. https://doi.org/https://ieeexplore.ieee.org/document/1304847

Dehghanipour, A.H., Zahabiyoun, B., Schoups, G., Babazadeh, H., 2019. A WEAP-MODFLOW surface water-groundwater model for the irrigated Miyandoab plain, Urmia lake basin, Iran: Multi-objective calibration and quantification of historical drought impacts. Agric. Water Manag. 223, 105704. https://doi.org/10.1016/j.agwat.2019.105704

Dunn, S.M., Stalham, M., Chalmers, N., Crabtree, B., 2003. Adjusting irrigation abstraction to minimise the impact on stream flow in the east of Scotland. J. Environ. Manage. 68, 95–107. https://doi.org/10.1016/S0301-4797(03)00006-9

Fallah-Mehdipour, E., Bozorg-Haddad, O., Loáiciga, H.A., 2020. Climate-environment-water: integrated and non-integrated approaches to reservoir operation. Environ. Monit. Assess. 192. https://doi.org/10.1007/s10661-019-8039-2

Fallah-Mehdipour, E., Bozorg-Haddad, O., Loáiciga, H.A., 2018. Calculation of multi-objective optimal tradeoffs between environmental flows and hydropower generation. Environ. Earth Sci. 77. https://doi.org/10.1007/s12665-018-7645-6

Farrokhzadeh, S., Monfared, S.A.H., Azizian, G., Shahraki, A.S., Ertsen, M.W., Abraham, E., 2020. Sustainable Water Resources Management in an Arid Area Using a Coupled Optimization-Simulation Modeling. Water 2020, Vol. 12, Page 885 12, 885. https://doi.org/10.3390/W12030885

Ghaheri, M., Baghal-Vayjooee, M.H., Naziri, J., 1999. Lake Urmia, Iran: A summary review. Int. J. Salt Lake Res. 8, 19–22. https://doi.org/10.1023/A:1009062005606

Hakami-Kermani, A., Babazadeh, H., Porhemmat, J., Sarai-Tabrizi, M., 2020. An uncertainty assessment of reservoir system performance indices under the climate change effect. Ain Shams Eng. J. https://doi.org/10.1016/j.asej.2020.03.015

Harbaugh, A.W., 2005. MODFLOW-2005, the US Geological Survey modular ground-water model: the ground-water flow process. US Department of the Interior, US Geological Survey.

Hosseini-Moghari, S.-M., Araghinejad, S., Tourian, M.J., Ebrahimi, K., Döll, P., 2018. Quantifying the impacts of human water use and climate variations on recent drying of Lake Urmia basin: the value of different sets of spaceborne and in-situ data for calibrating a hydrological model. Hydrol. Earth Syst. Sci. Discuss. 1–29. https://doi.org/10.5194/hess-2018-318

Hu, Z., Chen, Y., Yao, L., Wei, C., Li, C., 2016. Optimal allocation of regional water resources: From a perspective of equity-efficiency tradeoff. Resour. Conserv. Recycl. 109, 102–113. https://doi.org/10.1016/j.resconrec.2016.02.001

Jägermeyr, J., Pastor, A., Biemans, H., Gerten, D., 2017. Reconciling irrigated food production with environmental flows for Sustainable Development Goals implementation. Nat. Commun. 8. https://doi.org/10.1038/ncomms15900

Karamouz, M., Kerachian, R., Zahraie, B., 2004. Monthly water resources and irrigation planning: case study of conjunctive use of surface and groundwater resources. J. Irrig. … 391–402. https://doi.org/10.1061/(ASCE)0733-9437(2004)130:5(391)

Lemoalle, J., Bader, J.C., Leblanc, M., Sedick, A., 2012. Recent changes in Lake Chad: Observations, simulations and management options (1973-2011). Glob. Planet. Change 80–81, 247–254. https://doi.org/10.1016/j.gloplacha.2011.07.004

Loucks, D.P., van Beek, E., 2005. Appendix A : Natural System Processes and Interactions, Water Resources.

Mainuddin, M., Kirby, M., Qureshi, M.E., 2007. Integrated hydrologic-economic modelling for analyzing water acquisition strategies in the Murray River Basin. Agric. Water Manag. 93, 123–135. https://doi.org/10.1016/j.agwat.2007.06.011

Malano, H.M., Davidson, B., 2009. A framework for assessing the trade-offs between economic and environmental uses of water in a river basin. Irrig. Drain. 58, S133–S147. https://doi.org/10.1002/ird.484

Mancosu, N., Snyder, R.L., Kyriakakis, G., Spano, D., 2015. Water scarcity and future challenges for food production. Water (Switzerland) 7, 975–992. https://doi.org/10.3390/w7030975

Ministry of Energy of Iran, 2016. Implementation strategies for 40% reduction of Agricultural Water Consumption in Zarrineh Rood and Simineh rood River basins, Vol. 7: Planning and management studies of water resources and consumption in Miyandoab plain (available in Persian).

Molden, D., 2013. Water for food water for life: A Comprehensive assessment of water management in agriculture, Water for Food Water for Life: A Comprehensive Assessment of Water Management in Agriculture. https://doi.org/10.4324/9781849773799

Moshir Panahi, D., Kalantari, Z., Ghajarnia, N., Seifollahi-Aghmiuni, S., Destouni, G., 2020. Variability and change in the hydro-climate and water resources of Iran over a recent 30-year period. Sci. Rep. 10, 1–9. https://doi.org/10.1038/s41598-020-64089-y

Munoz-Hernandez, A., Mayer, A.S., Watkins, D.W., 2011. Integrated Hydrologic-Economic-Institutional Model of Environmental Flow Strategies for Rio Yaqui Basin, Sonora, Mexico. J. Water Resour. Plan. Manag. 137, 227–237. https://doi.org/10.1061/(ASCE)WR.1943-5452.0000108

Nalbantis, I., Tsakiris, · G, 2009. Assessment of Hydrological Drought Revisited. Water Resour Manag. 23, 881–897. https://doi.org/10.1007/s11269-008-9305-1

O'Keeffe, J., 2009. Sustaining river ecosystems: Balancing use and protection. Prog. Phys. Geogr. 33, 339–357. https://doi.org/10.1177/0309133309342645

Pang, A., Sun, T., Yang, Z., 2014. Cadre de détermination des débits environnementaux recommandé conciliant les demandes en eau agricoles et les écosystèmes. Hydrol. Sci. J. 59, 890–903. https://doi.org/10.1080/02626667.2013.816425

Pang, A., Sun, T., Yang, Z., 2013. Economic compensation standard for irrigation processes to safeguard environmental flows in the Yellow River Estuary, China. J. Hydrol. 482, 129–138. https://doi.org/10.1016/j.jhydrol.2012.12.050

Peralta, R.C., Cantiller, R.R.A., Terry, J.E., 1995. Optimal Large-Scale Conjunctive Water-Use Planning: Case Study. J. Water Resour. Plan. Manag. 121, 471–478. https://doi.org/10.1061/(ASCE)0733-9496(1995)121:6(471)

Pritchard, H.D., 2017. Asia's glaciers are a regionally important buffer against drought. Nature 545. 2017, 169-174, https://doi.org/10.1038/nature22062

Pulido-Velazquez, M., Andreu, J., Sahuquillo, A., Pulido-Velazquez, D., 2008. Hydro-economic river basin modelling: The application of a holistic surface-groundwater model to assess opportunity costs of water use in Spain. Ecol. Econ. 66, 51–65. https://doi.org/10.1016/j.ecolecon.2007.12.016

Purkey, D., Galbraith, H., Huber-Lee, A., Sieber, J., Yates, D., 2009. WEAP21—A Demand-, Priority-, and Preference-Driven Water Planning Model. Water Int. 30, 501–512. https://doi.org/10.1080/02508060508691894

Raes, D., Geerts, S., Kipkorir, E., Wellens, J., Sahli, A., 2005. Simulation of yield decline as a result of water stress with a robust soil water balance model. https://doi.org/10.1016/j.agwat.2005.04.006

Rumbaur, C., Thevs, N., Disse, M., Ahlheim, M., Brieden, A., Cyffka, B., Duethmann, D., Feike, T., Frör, O., Gärtner, P., Halik, Hill, J., Hinnenthal, M., Keilholz, P., Kleinschmit, B., Krysanova, V., Kuba, M., Mader, S., Menz, C., Othmanli, H., Pelz, S., Schroeder, M., Siew, T.F., Stender, V., Stahr, K., Thomas, F.M., Welp, M., Wortmann, M., Zhao, X., Chen, X., Jiang, T., Luo, J., Yimit, H., Yu, R., Zhang, X., Zhao, C., 2015. Sustainable management of river oases along the Tarim River (SuMaRiO) in Northwest China under conditions of climate change. Earth Syst. Dyn. 6, 83–107. https://doi.org/10.5194/esd-6-83-2015

Safavi, H.R., Darzi, F., Mariño, M.A., 2010. Simulation-optimization modeling of conjunctive use of surface water and groundwater. Water Resour. Manag. 24, 1965–1988. https://doi.org/10.1007/s11269-009-9533-z

Schoups, G., Addams, C.L., Gorelick, S.M., 2005. Multi-objective calibration of a surface water-groundwater flow model in an irrigated agricultural region: Yaqui Valley, Sonora, Mexico. Hydrol. Earth Syst. Sci. 9, 549–568. https://doi.org/10.5194/hess-9-549-2005

Schoups, G., Addams, C.L., Minjares, J.L., Gorelick, S.M., 2006. Sustainable conjunctive water management in irrigated agriculture: Model formulation and application to the Yaqui Valley, Mexico. Water Resour. Res. 42. https://doi.org/10.1029/2006WR004922

Schroeder, P.R., Dozier, T.S., Zappi, P.A., Mcenroe, B.M., Sjostrom, J.W., Peyton, R.L., 1994. The hydrologic evaluation of landfill performance (Help) model.

Schulz, S., Darehshouri, S., Hassanzadeh, E., Tajrishy, M., Schüth, C., 2020. Climate change or irrigated agriculture – what drives the water level decline of Lake Urmia. Sci. Rep. 10, 1–10. https://doi.org/10.1038/s41598-019-57150-y

Seo, S.B., Mahinthakumar, G., Sankarasubramanian, A., Kumar, M., 2018. Conjunctive Management of Surface Water and Groundwater Resources under Drought Conditions Using a Fully Coupled Hydrological Model. J. Water Resour. Plan. Manag. 144, 04018060. https://doi.org/10.1061/(ASCE)WR.1943-5452.0000978

Shadkam, S., Ludwig, F., van Vliet, M.T.H., Pastor, A., Kabat, P., 2016. Preserving the world second largest hypersaline lake under future irrigation and climate change. Sci. Total Environ. 559, 317–325. https://doi.org/10.1016/j.scitotenv.2016.03.190

Sieber, J., Purkey, D., 2015. WEAP Water Evaluation and Planning System: User Guide, Stockholm Environment Institute, US Center.

Singh, A., 2014. Simulation-optimization modeling for conjunctive water use management. Agric. Water Manag. 141, 23–29. https://doi.org/10.1016/j.agwat.2014.04.003

Singh, A., Panda, S.N., 2013. Optimization and Simulation Modelling for Managing the Problems of Water Resources. Water Resour. Manag. 27, 3421–3431. https://doi.org/10.1007/s11269-013-0355-7

Sisto, N.P., 2009. Environmental flows for rivers and economic compensation for irrigators. J. Environ. Manage. 90, 1236–1240. https://doi.org/10.1016/j.jenvman.2008.06.005

Smakhtin, V.U., Shilpakar, R.L., Hughes, D.A., 2006. Hydrology-based assessment of environmental flows: An example from Nepal. Hydrol. Sci. J. 51, 207–222. https://doi.org/10.1623/hysj.51.2.207

Srinivasa Prasad, A., Umamahesh, N. V., Viswanath, G.K., 2006. Optimal irrigation planning under water scarcity. J. Irrig. Drain. Eng. 132, 228–237. https://doi.org/10.1061/(ASCE)0733-9437(2006)132:3(228)

Tennant, D.L., 1976. Instream Flow Regimens for Fish, Wildlife, Recreation and Related Environmental Resources. Fisheries 1, 6–10. https://doi.org/10.1577/1548-8446(1976)001<0006:ifrffw>2.0.co;2

Tharme, R.E., 2003. A global perspective on environmental flow assessment: Emerging trends in the development and application of environmental flow methodologies for rivers. River Res. Appl. 19, 397–441. https://doi.org/10.1002/rra.736

Tian, Y., Zheng, Y., Zheng, C., Xiao, H., Fan, W., Zou, S., Wu, B., Yao, Y., Zhang, A., Liu, J., 2015. Exploring scale-dependent ecohydrological responses in a large endorheic river basin through integrated surface water-groundwater modeling. Water Resour. Res. 51, 4065–4085. https://doi.org/10.1002/2015WR016881

Valipour, M., 2015. A comprehensive study on irrigation management in Asia and Oceania. Arch. Agron. Soil Sci. 61, 1247–1271. https://doi.org/10.1080/03650340.2014.986471

Valipour, M., Ziatabar Ahmadi, M., Raeini-Sarjaz, M., Gholami Sefidkouhi, M.A., Shahnazari, A., Fazlola, R., Darzi-Naftchali, A., 2015. Agricultural water management in the world during past half century. Arch. Agron. Soil Sci. 61, 657–678. https://doi.org/10.1080/03650340.2014.944903

Wang, J., Song, C., Reager, J.T., Yao, F., Famiglietti, J.S., Sheng, Y., MacDonald, G.M., Brun, F., Schmied, H.M., Marston, R.A., Wada, Y., 2018. Recent global decline in endorheic basin water storages. Nat. Geosci. 11, 926–932. https://doi.org/10.1038/s41561-018-0265-7

Wei, Y., Davidson, B., Chen, D., White, R., 2009. Balancing the economic, social and environmental dimensions of agro-ecosystems: An integrated modeling approach. Agric. Ecosyst. Environ. 131, 263–273. https://doi.org/10.1016/j.agee.2009.01.021

Xevi, E., Khan, S., 2005. A multi-objective optimisation approach to water management. J. Environ. Manage. 77, 269–277. https://doi.org/10.1016/j.jenvman.2005.06.013

Xue, J., Gui, D., Lei, J., Sun, H., Zeng, F., Feng, X., 2017. A hybrid Bayesian network approach for trade-offs between environmental flows and agricultural water using dynamic discretization. Adv. Water Resour. 110, 445–458. https://doi.org/10.1016/j.advwatres.2016.10.022

Yang, W., Yang, Z., 2014. Analyzing hydrological regime variability and optimizing environmental flow allocation to lake ecosystems in a sustainable water management framework: Model development and a case study for china’s baiyangdian watershed. J. Hydrol. Eng. 19, 993–1005. https://doi.org/10.1061/(ASCE)HE.1943-5584.0000874

Yapiyev, V., Sagintayev, Z., Inglezakis, V.J., Samarkhanov, K., Verhoef, A., 2017. Essentials of endorheic basins and lakes: A review in the context of current and futurewater resource management and mitigation activities in Central Asia. Water (Switzerland) 9, 798. https://doi.org/10.3390/w9100798

Yasi, M., Ashori, M., 2017. Environmental Flow Contributions from In-Basin Rivers and Dams for Saving Urmia Lake. Iran. J. Sci. Technol. Trans. Civ. Eng. 41, 55–64. https://doi.org/10.1007/s40996-016-0040-1

Supplementary material to

Meeting agricultural and environmental water demand in endorheic irrigated river basins: a simulation-optimization approach applied to the Urmia Lake basin in Iran

Amir Hossein Dehghanipour[a,*,1], Gerrit Schoups[b], Bagher Zahabiyoun [a,*], Hossein Babazadeh[c]

[a] Department of Water Management, School of Civil Engineering, Iran University of Science and Technology, Tehran, Iran
[b] Department of Water Management, Faculty of Civil Engineering and Geosciences, Delft University of Technology, Delft, The Netherlands
[c] Department of Water Science and Engineering, Science and Research Branch, Islamic Azad University, Tehran, Iran

[*] Corresponding author address: Department of Water Management, School of Civil Engineering, Iran University of Science and Technology, Narmak, Tehran, Iran, Postal Code: 16846-13114.
E-mail: A.Dehghanipour@tudelft.nl (A.H. Dehghanipour), Bagher@iust.ac.ir (B. Zahabiyoun)

[1]Present address: Department of Water Management, Faculty of Civil Engineering and Geosciences, Delft University of Technology, Stevinweg 1, 2628CN, Delft, Netherlands.

1.Introduction

The supplementary material includes additional Figures (Fig. S1 to S7), Tables (Table S1 to S6), and text to enhance our article. Table S1 presents a summary of previous studies that applied simulation-optimization to find water allocation strategies that simultaneously meet environmental flow requirements and water demand from agriculture and other users. Table S2, Table S3, and Fig. S1 present crop characteristics for the Miyandoab Plain and Fig. S2 shows the annual observed river discharge upstream of Bukan reservoir. Finally, Fig. S3 to S7 and Table S4 to S6 provide additional information on results and discussion in the paper.

Table S1: Some studies applied the optimization model to evaluate environmental flow requirements

Study	Objective Function	Case study	Environmental flow requirement	
			Implementation in the optimization	Calculation method
Xevi and Khan (2005)	• maximize agricultural net profit • minimize variable cost • minimize total groundwater withdrawal to meet agricultural demand	hypothetical Irrigation Area using real data of Berembed Weir on the Murrumbidgee River in Australia	As a firm constraint	Downstream measured river discharge
Pulido-Velazquez et al. (2008)	• minimize the total cost of water distribution and system operation in the agricultural and urban sectors	Adra River Basin in Spain	as a firm constraint	Unknown
Anghileri et al. (2013)	• minimize deficit irrigation • maximize hydropower generation	Alpine watershed in Italy	as a firm constraint	function of the reservoir storage
Yang and Yang (2014)	• maximize the net benefit for the industrial sectors • minimize the absolute deviation of the calculated lake water level from the natural level • minimize the crop yield losses	Lake Baiyangdian basin in China	as an objective function	was not considered
Roozbahani et al. (2015)	• maximize the profit of agricultural, urban, and industrial sectors • minimize the shortage of supply environmental flow requirements • maximizes allocated water to the social aspect	Sefidrud Basin in Iran	as an objective function	Using Tennant method
Hu et al. (2016)	• maximize the economic benefit efficiency from water allocation • maximize water allocation equity by using the Gini coefficient	Qujiang river basin in China	as a firm constraint	Using Tennant method
Fallah-Mehdipour et al. (2018)	• minimized deviation between the installed capacity of the power plant and generated power • minimized the absolute difference between the environmental flow requirement and reservoir release	Karoon Basin in Iran	as an objective function	Using Tennant method
Fallah-Mehdipour et al. (2020)	• maximize supply water for agricultural demand • maximize supply water for environmental flow requirements • maximize supply water for urban demand	Karkhe Basin in southwestern Iran	as an objective function	Using Tennant method
Our study	• maximize agricultural net profit • maximize agricultural sustainability • maximize inflow to the Lake	Urmia lake basin in Iran	as an objective function	Decision variable in the optimization model

2. Case study

Table S2: Growing Stage Length, Crop coefficients (k_c), and Maximum root depth for crops in Miyandoab Plain according to FAO Irrigation and Drainage (Allen et al., 1998)

Crop or Orchards	Stage Length (day)				k_c			Root Depth (m)	ETp (m^3/hec)
	Initial	Development	Midseason	Late	Initial	Midseason	Late		
Alfalfa (1st cutting cycle)	10	30	25	10	0.4	0.95	0.9	1.5	8730.36
Alfalfa (2st, 3st, 4st cutting cycle)	5	20	10	10	0.4	0.95	0.9	1.5	
Wheat	30	140	40	30	0.4	1.15	0.3	1.65	5199.79
Maize	25	40	45	30	0.15	1.2	0.5	1.35	6373.55
Tomato	25	40	60	30	0.15	1.15	0.8	1.1	6701.28
Sugar beet	35	60	70	40	0.35	1.2	0.7	0.95	9048.52
Canola	20	120	30	30	0.35	1.2	0.35	1.25	3248.65
Sorghum	25	35	40	30	0.4	1.1	0.75	1.5	5336.50
Saffron	30	45	70	55	0.4	0.85	0.55	0.45	2922.84

Table S3: Maximum yield (Ym), market price, and cost of crops in Miyandoab Plain (Ministry of Energy of Iran, 2016). Yields and prices are listed for first (e.g. grain) and second (e.g. straw) harvests.

Crop	First harvest		Second harvest		Cost (USD/ha)	Maximum net profit (USD/ha)
	Yield Y_{m1} (Kg/ha)	Market price 1 (USD/Kg)	Yield Y_{m2} (Kg/ha)	Market price 2 (USD/Kg)		
Wheat	5500	0.46	6600	0.08	797.96	2260
Maize	10300	0.38	5950	0.06	1288.92	3023
Alfalfa	13000	0.32	0	0	1365.2	2795
Tomato	50000	0.14	0	0	3229.2	3771
Sugar beet	70000	0.11	0	0	3001.76	4558
Canola	3100	0.88	2402	0.08	950.8	1969
Sorghum	97000	0.06	0	0	1322.92	4109
Saffron	10	2000	18948	0.04	3637.96	13120

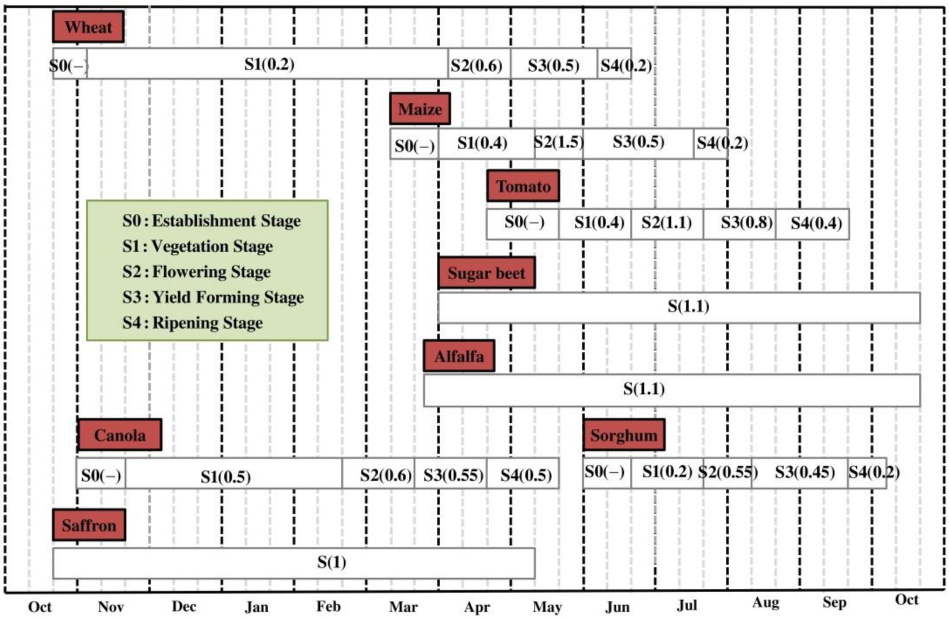

Fig. S1: Calendar and growth stages (S0-S4) for crops in the Miyandoab Plain. Values in brackets are the crop yield response factors ($k_{y,i}$ in Eq. 2) for each crop stage (Ministry of Energy of Iran, 2016; Steduto et al., 2012).

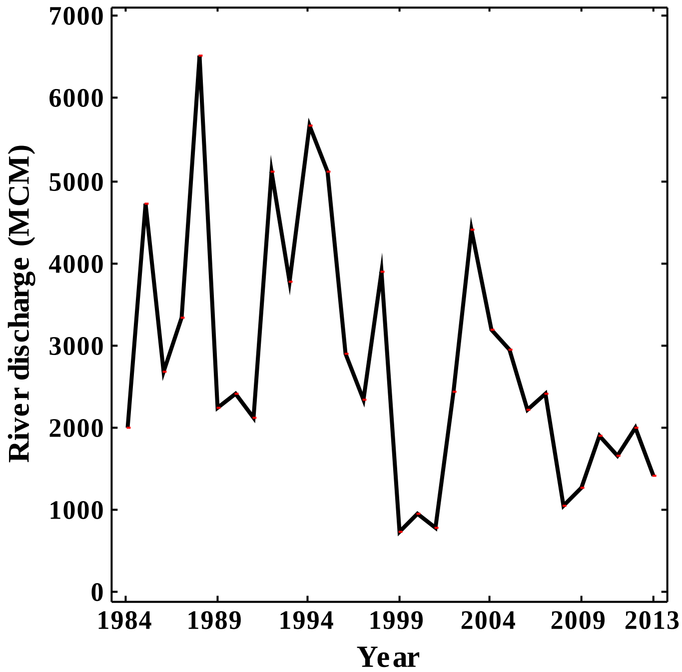

Fig. S2: Time series of annual observed river discharge upstream of Bukan reservoir

3.Results and discussion

The integrated simulation-optimization model includes 5000 simulation runs for each strategy. In this study, we used WEAP (version 2019), MODFLOW 2005, and MATLAB (version 2018) to develop the simulation-optimization model. Each simulation run for the period (1984-2013) takes on average 7 min on a standard desktop system with CPU speed of 3.7 GHz and 16 GB of memory installed (RAM).

Fig. S3.a and S3.b show heat maps of the intervention point (Z_{int}), i.e. relative soil water content that triggers irrigation, for each growth stage of each crop in current and proposed crop patterns in strategy I, respectively (for HD1 and HD2 years; crop acreages for HD3 years were near zero). As mentioned before, irrigation starts when relative soil water content falls below the intervention point. Therefore, decreasing the intervention point results in more deficit irrigation, less water withdrawal for irrigation, and more crop water stress. Value of the intervention point increases from scenarios 1 to 3 (scenarios 4 to 6). Therefore, water withdrawal for irrigation increases from scenarios 1 to 3 (scenarios 4 to 6) (Table S4 and Table S5), resulting in an increase of the Economic agricultural index and a decrease of the Environmental index (Fig. 7.a). Furthermore, the intervention point decreases from HD1 to HD2, i.e. drier conditions lead to more deficit irrigation.

The application of deficit irrigation varies by crop. Drought-resistant crops like wheat, with values for yield response factor K_y less than 1 in each growth stage (Fig. S1), are more suited for deficit irrigation, than drought-sensitive crops like sugar beet and saffron, with yield response factor values greater than 1. These crop differences are reflected in the optimal values of z_{int} in Fig. S3, which are high for sugar beet and saffron, and low for wheat.

Furthermore, the application of deficit irrigation is sensitive to the growth stage. For instance, the intervention point of stage 2 (vegetation stage) of maize and tomato is higher than other stages, because of the yield response factor (K_y) of this stage is higher than 1, and this stage is sensitive to deficit irrigation. On the other hand, the intervention points of stage 4 (ripening stage) of wheat, maize, and tomato are lower compared to other stages. The yield response factor (K_y) of this stage is smallest, and thus deficit irrigation is applied in stage 4.

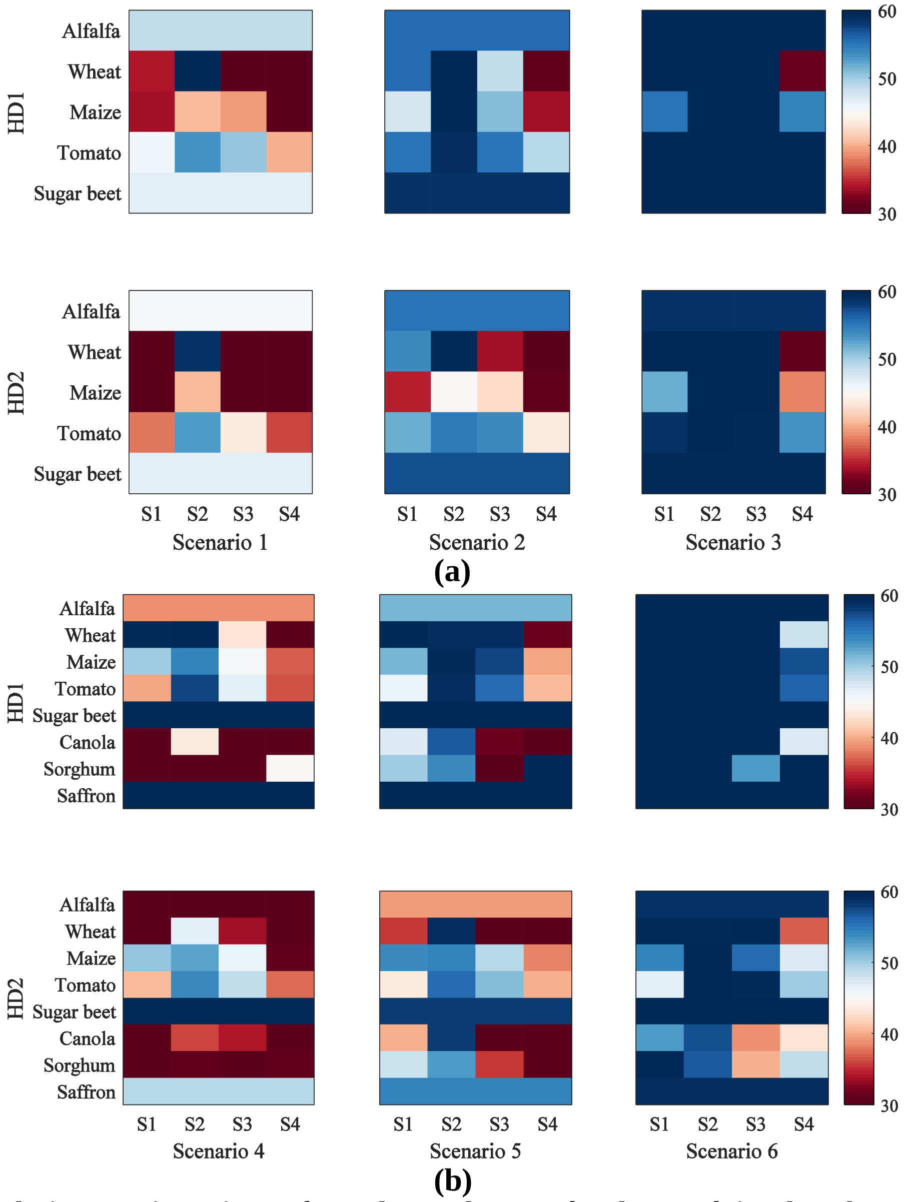

Fig. S3: Values for the intervention point z_{int} for each growth stage of each crop of six selected scenarios on the Pareto front of strategy I: (a) current crop pattern, and (b) proposed crop pattern. HD1, HD2, HD3 are hydrological conditions: non-drought, mild drought, and moderate drought, respectively. Historically, the value of z_{int} is 45%.

Table S4: Time-averaged (1984-2013) root-zone water balance components (in MCM) for agricultural zones within the Miyandoab aquifer boundary for the six Pareto scenarios of strategy I.

Parameter		Historical	scenario 1	scenario 2	scenario 3	scenario 4	scenario 5	scenario 6
Inflow	Effective precipitation	218.68	218.68	218.68	218.68	218.68	218.68	218.68
	SW extraction for irrigation	763.79	721.04	807.4	907.74	598.06	722.28	848.65
	GW extraction for irrigation	136.82	126.48	133.21	133.93	110.23	116.16	123.01
	Total inflows	1119.28	1066.2	1159.29	1260.35	926.97	1057.12	1190.34
Outflow	ET actual	366.26	347.39	368.15	373.81	315.03	330.67	349.64
	Surface runoff+Interflow	561.14	552.19	605.06	678.55	459.59	549.14	633.17
	GW recharge	182.67	166	180.53	191.25	148.43	166.45	186.25
	Total outflows	1110.06	1065.58	1153.75	1243.61	923.05	1046.27	1169.06
Storage change		9.22	0.62	5.54	16.74	3.92	10.85	21.27

Table S5: Simulated time-averaged (1984-2013) root-zone water balance components (in MCM) for agricultural zones outside of the Miyandoab aquifer boundary for six selected scenarios in the Pareto front in strategy I.

Parameter		Historical	Scenario 1	Scenario 2	Scenario 3	Scenario 4	Scenario 5	Scenario 6
Inflow	Effective precipitation	116.97	116.97	116.97	116.97	116.97	116.97	116.97
	SW extraction for irrigation	174.74	168.39	181.66	199.73	156.56	177.48	202.24
	GW extraction for irrigation	197.21	186.39	192.09	191.06	172.86	180.59	187.52
	Total inflows	488.92	471.75	490.72	507.76	446.4	475.05	506.73
Outflow	ET actual	185.09	180.69	183.82	185.96	172.52	176.7	181.55
	Surface runoff + Interflow	194.84	190.3	199.14	211.27	173.96	191.79	209.85
	GW recharge	107.5	102.21	106.47	108.98	99.95	105.12	110.51
	Total outflows	487.43	473.2	489.42	506.22	446.43	473.6	501.9
Storage change		1.49	-1.44	1.3	1.54	-0.03	1.44	4.82

Table S6: The value of GW capacity and crop acreage in HD3 in scenarios 7 to 9.

Variable		scenario 7	scenario 8	scenario 9
Area	HD1	similar scenario 4-HD1	similar scenario 5-HD1	similar scenario 6-HD1
	HD2	similar scenario 4-HD2	similar scenario 5-HD2	similar scenario 6-HD2
	HD3	Current Area	Current Area	Current Area
Zint	HD1	similar scenario 4-HD1	similar scenario 5-HD1	similar scenario 6-HD1
	HD2	similar scenario 4-HD2	similar scenario 5-HD2	similar scenario 6-HD2
	HD3	similar scenario 4-HD2	similar scenario 5-HD2	similar scenario 6-HD2
MFR		similar scenario 4	similar scenario 5	similar scenario 6
GW capacity	HD1	No change	No change	No change
	HD2	No change	No change	No change
	HD3	Increase until 2 time	Increase until 2 time	Increase until 2 time

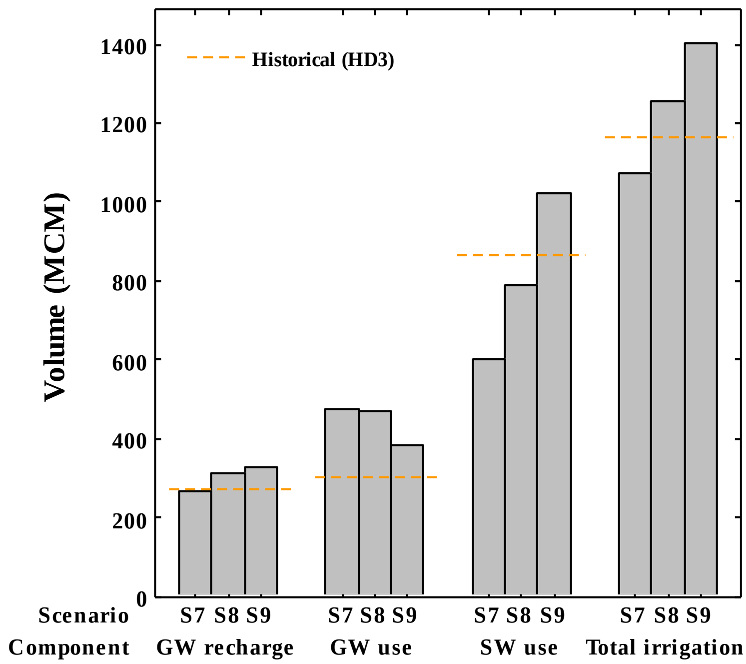

Fig. S4: Water balance components for scenarios 7-9 in HD3 years (moderate drought)

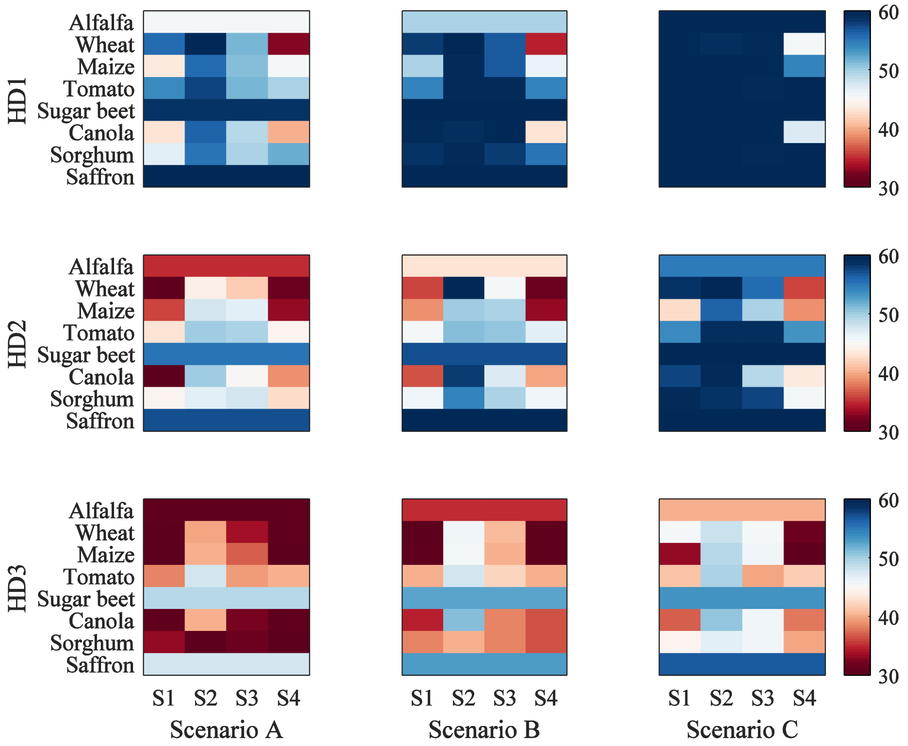

Fig. S5: Values for intervention point z_{int} for each growth stage of each crop of three selected scenarios on the Pareto front of strategy II

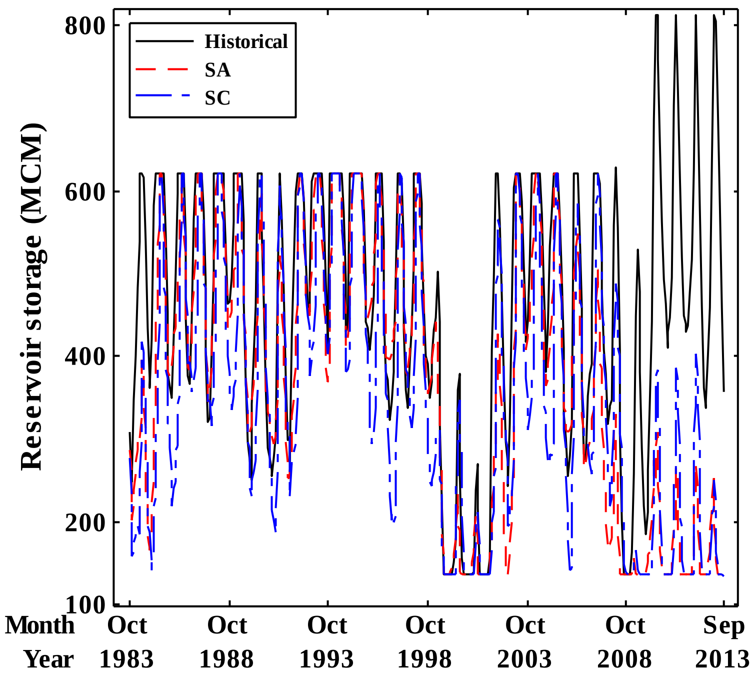

Fig. S6: Monthly Bukan reservoir storage for three selected scenarios on the Pareto front of strategy II.

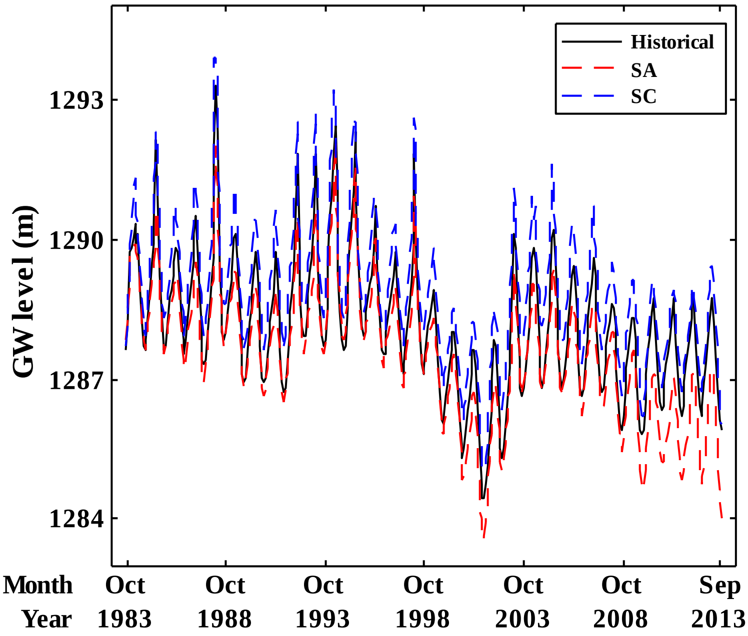

Fig. S7: Monthly GW levels for three selected scenarios on the Pareto front of strategy II.

References

Allen, R.G., Pereira, L.S., Raes, D., Smith, M., 1998. FAO Irrigation and drainage paper No. 56. Rome: Food and Agriculture Organization of the United Nations.

Anghileri, D., Castelletti, A., Pianosi, F., Soncini-Sessa, R., Weber, E., 2013. Optimizing watershed management by coordinated operation of storing facilities. J. Water Resour. Plan. Manag. 139, 492–500. https://doi.org/10.1061/(ASCE)WR.1943-5452.0000313

Fallah-Mehdipour, E., Bozorg-Haddad, O., Loáiciga, H.A., 2020. Climate-environment-water: integrated and non-integrated approaches to reservoir operation. Environ. Monit. Assess. 192. https://doi.org/10.1007/s10661-019-8039-2

Fallah-Mehdipour, E., Bozorg-Haddad, O., Loáiciga, H.A., 2018. Calculation of multi-objective optimal tradeoffs between environmental flows and hydropower generation. Environ. Earth Sci. 77. https://doi.org/10.1007/s12665-018-7645-6

Hu, Z., Chen, Y., Yao, L., Wei, C., Li, C., 2016. Optimal allocation of regional water resources: From a perspective of equity-efficiency tradeoff. Resour. Conserv. Recycl. 109, 102–113. https://doi.org/10.1016/j.resconrec.2016.02.001

Ministry of Energy of Iran, 2016. Implementation strategies for 40% reduction of Agricultural Water Consumption in Zarrineh Roud and Simineh rood River basins, Vol. 7: Planning and management studies of water resources and consumption in Miyandoab plain (available in Persian).

Pulido-Velazquez, M., Andreu, J., Sahuquillo, A., Pulido-Velazquez, D., 2008. Hydro-economic river basin modelling: The application of a holistic surface-groundwater model to assess opportunity costs of water use in Spain. Ecol. Econ. 66, 51–65. https://doi.org/10.1016/j.ecolecon.2007.12.016

Roozbahani, R., Schreider, S., Abbasi, B., 2015. Optimal water allocation through a multi-objective compromise between environmental, social, and economic preferences. Environ. Model. Softw. 64, 18–30. https://doi.org/10.1016/j.envsoft.2014.11.001

Steduto, P., Hsiao, T.C., Fereres, E., Raes, D., 2012. Crop yield response to water, FAO Irrigation and Drainage Paper No.66.

Xevi, E., Khan, S., 2005. A multi-objective optimisation approach to water management. J. Environ. Manage. 77, 269–277. https://doi.org/10.1016/j.jenvman.2005.06.013

Yang, W., Yang, Z., 2014. Analyzing hydrological regime variability and optimizing environmental flow allocation to lake ecosystems in a sustainable water management framework: Model development and a case study for china's baiyangdian watershed. J. Hydrol. Eng. 19, 993–1005. https://doi.org/10.1061/(ASCE)HE.1943-5584.0000874